NTNU – Trondheim
Norwegian University of
Science and Technology

Influence of HVDC with Overlaid Transients on the Life Time of Wet XLPE Cable Insulation

Halvor Hoen Hersleth

Master of Energy and Environmental Engineering
Submission date: June 2013
Supervisor: Frank Mauseth, ELKRAFT

Norwegian University of Science and Technology
Department of Electric Power Engineering

Problem Description

There are many technological challenges related to the production of electrical power from offshore wind farms. Numerous Norwegian companies are working on different aspects of offshore wind power generation as a result.

This master thesis is a part of the 5 year project “High Voltage AC and DC Subsea Cables for Offshore Wind Farms and Transmission Grids” supported by The Norwegian Research Council. The purpose of this master thesis is to study the ageing properties of subsea cable insulation with relevant voltage stresses applied. Power electronics used for HVDC converters will stress the cable with a HVDC voltage with overlaid transients. The effect of these transients on the performance of the polymeric cable insulation is not yet known. The main objective of the master thesis is to investigate how transients can influence water tree growth within wet XLPE insulation.

The master thesis is mainly experimental. Experiments will be carried out on Rogowski shaped test objects exposed to a DC voltage with a superimposed high frequency AC component, approximating the voltage stress a HVDC cable will experience as a result of the power electronic converters. Water tree initiation and growth will be investigated as a function of time. The effect of the DC voltage on water tree degradation will also be investigated.

Acknowledgements

This report is a result of work with the master thesis conducted at the Norwegian University of Science and Technology, NTNU, at the Department of Electric Power Engineering, in coordination with SINTEF.

I would like to thank my supervisor at NTNU, Frank Mauseth, for constructive feedback, passionate support, and much appreciated guidance during all parts of my master thesis. I would also like to thank my fellow students, at room F-452, for good advice, motivation and fruitful conversations.

07.06.2013

Halvor Hoen Hersleth

Abstract

There are many technological challenges related to the production of electrical power from offshore wind farms. Norwegian companies are working on different aspects of offshore wind power generation and the Norwegian Research Council has in this context supported a five year project called: “High Voltage AC and DC Subsea Cables for Offshore Wind Farms and Transmission Grids”. This master thesis has been a part of that project.

Power electronics used for HVDC converters will stress the cable with a HVDC component with overlaid transients. The effect of the DC component and the overlaid transients on the performance of the polymeric cable insulation is not yet known and the main purpose of this master thesis has been to investigate how transients can influence water tree growth within wet XLPE insulation. The effect of the DC component has also been evaluated.

Laboratory experiments were conducted on Rogowski shaped test objects with an insulation thickness of 1.1 mm. 20 sodium chloride particles were added on the lower semiconductor during the manufacturing process. This was done to facilitate the initiation of water trees. The finished test objects were preconditioned with demineralized water in a heating cabinet at 30 °C for four weeks to ensure that the insulation was saturated with water.

An experimental setup capable of applying a DC voltage with a superimposed high frequency AC component was used to simulate the HVDC component and the overlaid transients that occur close to the power electronics used for AC to DC conversion. Two sets of experiments were conducted. The first set was conducted using a 15 kHz AC component, with resulting electrical field strength of ± 2.05 kV/mm. The second set of experiments was conducted combining the same high frequency AC component with a superimposed DC voltage, resulting in an electrical field strength of 12 ± 2.05 kV/mm. Nine Rogowski shaped test objects were aged in both sets of experiments. Three test objects were aged for one week, another three for two weeks, while the last three test objects were aged for three complete weeks. The test objects were kept in a heating cabinet at 30 °C during testing, and with the exception of the electrical field, treated identically during both sets of experiments.

All test objects experienced water tree initiation and growth. The length of the longest water tree and the aggregated water tree density were observed to increase as a function of ageing time for both sets of experiments. All water trees were oblong and grew in the direction of the electrical field. The longest observed water tree, after three weeks of ageing exposed to an AC component only, was 607 µm, corresponding to 55 % of the total insulation thickness. Two out of three test objects, exposed to a DC voltage with a superimposed AC component, suffered breakdown before enduring three complete weeks of ageing. This was most likely the result of a water tree bridging the 1100 µm thick insulation. Test objects exposed to a DC voltage with a superimposed high frequency AC component were also observed to experience a higher aggregated water tree density, with vented water trees observed at the lower semiconductor constituting the main difference. As a result, it could be argued that the DC voltage, when combined with a superimposed high frequency AC component, increases water tree initiation and growth within wet XLPE insulation. The experiments also indicate that HVDC cables should be made water tight to prevent water tree degradation due to the transients originating from the switching of the power electronic converters.

Sammendrag

Det er mange tekniske utfordringer knyttet til produksjon av elektrisk kraft fra offshore vindparker. Mange norske bedrifter jobber med de forskjellige aspektene knyttet til offshore vind og Norges forskningsråd har i den forbindelse tildelt SINTEF Energi femårsprosjektet: “High Voltage AC and DC Subsea Cables for Offshore Wind Farms and Transmission Grids”. Denne masteroppgaven er en del av dette prosjektet.

Kraftelektronikk brukt i likerettere vil belaste likestrømkabelen med en likespenning med overlagrede transienter. Effekten av denne påkjenningen på kabelisolasjonen er ukjent og hovedformålet med denne masteroppgaven har vært å undersøke hvordan transienter kan påvirke vanntrevekst i våt PEX-isolasjon, samt å undersøke innvirkningen til likespenningskomponenten.

Laboratorieforsøk ble gjennomført på Rogowski-formede testobjekt med en isolasjonstykkelse på 1.1 mm. 20 saltpartikler ble tilført kontaktflaten mellom den nedre halvlederen og isolasjonen under fabrikasjonsprosessen. Dette ble gjort for å framskynde initiering og vekst av vanntær. For å sikre at hele isolasjonen var mettet med vann før testing ble de ferdige testobjektene fylt med demineralisert vann og prekondisjonert i et varmeskap ved 30 °C i fire uker.

Et eksperimentelt oppsett med muligheten til å påføre en likespenning med en superponert høyfrekvent vekselspenningskomponent ble brukt for å simulere likespenningen og de overlagrede transientene som inntreffer nærme kraftelektronikk brukt i likerettere. To sett med forsøk ble utført. Det første settet med forsøk ble utført med en høyfrekvent vekselspenningskomponent, med en resulterende elektrisk feltstyrke på ± 2.05 kV/mm. Den andre runden med forsøk ble gjennomført ved å kombinere den samme høyfrekvente vekselspenningskomponenten med en likespenningskomponent. Dette resulterte i en elektrisk feltstyrke på of 12 ± 2.05 kV/mm. Ni Rogowski-formede testobjekt ble testet i begge settene med forsøk. Tre testobjekt ble fjernet fra oppsettet etter en uke med aldring, tre til etter to uker med aldring og de siste tre testobjektene ble fjernet etter tre uker med aldring. Testobjektene ble oppbevart i et varmeskap ved 30 °C under testing og ble med unntak av den elektriske feltstyrken, behandlet helt likt.

Initiering og vekst av vanntrær ble observert i alle testobjekt. Lengden på det lengste vanntreet og det totale antallet av vanntrær i isolasjonen ble for begge forsøk observert å øke som en funksjon av tiden. Alle vanntrær var avlange og vokste i retningen til det elektriske feltet. Det lengste observerte vantreet etter tre uker med aldring eksponert til bare en vekselsspenningkomponent var 607 µm, noe som utgjorde 55 % av den totale isolasjonstykkelsen. To av de tre testobjektene som skulle aldres i tre uker, eksponert til likespenning og en superponert høyfrekvent vekselspenningskomponent, fikk gjennomslag i isolasjonen. Dette var mest sannsynlig et resultat av vanntrær som vokste gjennom hele isolasjonen, altså 1100 µm. Testobjekt utsatt for en likespenning med en superponert høyfrekvent vekselspenningkomponent ble også observert å erfare en høyere vanntretetthet, med vanttrær initiert fra den nedre halvleder som den største forskjellen. Som en følge av dette, kan det argumenteres med at likespenning, kombinert med en superponert høyfrekvent vekselspenning, fremmer vanntrevekst i våt PEX-isolasjon. Forsøkene indikerer også at likestrømskabler med PEX-isolason burde produseres vanntette for å unngå vanntrevekst som følge av de overlagrede transientene som inntreffer nærme kraftelektronikk brukt i likerettere.

Table of Contents

1. Introduction

The threat of global warming and the anticipated decline in fossil fuel supply have initiated a revolution within the European energy sector and resulted in binding policies such as the EU 2020 target. Wind power, and especially offshore wind has emerged as one of the fastest growing sectors within renewable power production and is expected to contribute greatly towards the EU 2020 target. Large scale offshore wind farms are being implemented all across Europe, but there are still many issues and deal breakers within the industry. Numerous Norwegian companies are working on different aspects of offshore wind power generation and this master thesis is a part of the 5 year project; “High Voltage AC and DC Subsea Cables for Offshore Wind Farms and Transmission Grids”, supported by The Norwegian Research Council.

Offshore power transmission is considered one of the main bottlenecks within the offshore wind power industry. Due to the increasing distance from shore, HVDC is going to be the power transmission system of choice for many of the new offshore wind farms. The newer VSC HVDC technology is preferable as a result of black start capability, better reactive power control and a significant reduction of harmonics. However, the resulting HVDC voltage from the rectifier will still contain transients originating from the switching of the power electronic components. These harmonics can be lowered by installing filters, but this solution is often limited by the offshore converter station’s space and cost limitations. The insulation in close proximity to the converter will experience the most severe harmonics due to dampening along the cable. This part of the cable also experiences the largest mechanical strain, with the cable connection often designed to be quite flexible, facilitating the connection to the offshore converter station, and to some degree, reducing the mechanical strain on the cable. This does however also reduce the armoring of the cable, making this part of the cable more prone to water shielding fracture, which can lead to water intrusion, and as a result of the high frequency harmonics, facilitate water tree initiation and growth.

Water treeing is a degradation mechanism creating structures in polymer insulation under the influence of humidity and AC stress. Water trees can grow across and bridge the insulation, resulting in breakdown. Water trees can also facilitate the initiation of electrical trees, which in turn can lead to partial discharges and breakdown in the insulation. This means that water treeing can reduce the lifetime of XLPE insulated cables.

The research conducted was mainly experimental. Rogowski type test objects were manufactured in a plastic lab, with salt particles added on the lower semiconductor to facilitate the initiation of water trees. Experiments were then conducted using an experimental setup capable of applying a DC voltage with a superimposed high frequency AC voltage, thus simulating the HVDC component and the overlaid transients that occur close to the power electronics used for HVDC converters. Two sets of experiments were conducted. The first experiments were conducted using the high frequency AC component only, while the second round of experiments combined the same high frequency AC component, with a DC component. The two sets of results were compared, with water tree initiation and growth being investigated as a function of time.

This master thesis consists of four main parts. The first part is made up of chapter 2 and 3. These chapters form the backbone of the master thesis, including background on offshore wind and HVDC power transmission, as well as a theory chapter on electrical water treeing. Part two consists of chapter 4, which describes the preparation of the Rogowski shaped test objects, the experimental setup, and how the experiments were conducted. Part three consists of chapter 5 and 6, with chapter 5 presenting the experimental results, and chapter 6 covering the assessment of the results and the following discussion. Part four consists of chapter 7, the conclusion, and chapter 8, a suggestion for further studies and research. This last part concludes the master thesis.

2. Background

2.1. Offshore Wind

Coal and gas powered power plants have been the main source of electrical power generation worldwide for the last decades. The threat of global warming and the anticipated decline in fossil fuel reserves have started a revolution within the energy sector. In Europe, the EU 2020 target, has emerged as the most influential energy policy on the matter and is considered one of the main European drivers for renewable energy expansion [1]. The EU 2020 target has been put forth to limit global warming, reduce the dependence on oil, gas and coal within the energy sector, and to facilitate lower energy prices all over Europe. The main objectives are; for each participating country to have a 20% renewable energy generation in the gross consumption, to increase energy efficiency by 20%, and to reduce greenhouse gas emission by 20% compared to the 1990-levels. All three goals are legally binding and have accelerated the massive growth within the renewable energy sector in Europe.

Wind power, and especially offshore wind power, has emerged as one of the fastest growing sectors within renewable energy and is expected to contribute greatly towards the EU 2020 target. Large scale offshore wind is being and has already been implemented in Germany, Denmark and The United Kingdom, and is in many cases preferable to onshore wind due to factors such as higher and more stable wind conditions, geographic locations and less visual pollution. The trend within the offshore wind industry implies larger wind farms, further from shore, with the Dogger Bank project in the UK being a perfect example [2]. As a result of this, offshore power transmission is being considered one of the main bottlenecks within the offshore wind power industry.

Both high voltage alternating current (HVAC) and high voltage direct current (HVDC) are viable solutions for offshore wind farms. Long HVAC cables are affected by capacity charging and need extensive and expensive compensation at longer distances. This has led to HVDC being increasingly used for offshore power transmission over long distances. With a break even distance of about 70-100 km, depending on various conditions, but mainly the distance from shore, HVDC is going to be the power transmission system of choice for many new offshore wind farms [3].

2.2. HVDC Converter Technology

A basic HVDC system consists of two converter stations, one at each end, and a DC circuit between the two stations. AC voltage and current is supplied into one of the converter stations, where a rectifier converts AC to DC. The DC power is then transferred through the DC circuit and to the receiving end, which is connected to the other converter station. Here, an inverter converts the DC power back into AC power, which is supplied into the grid. Figure 2.1, on the next page, shows the basic topology of a HVDC transmission system. Two different types of HVDC technology are available on the market, with the main difference being the choice of converters [3]. The two different converters are current source converters and voltage source converters.

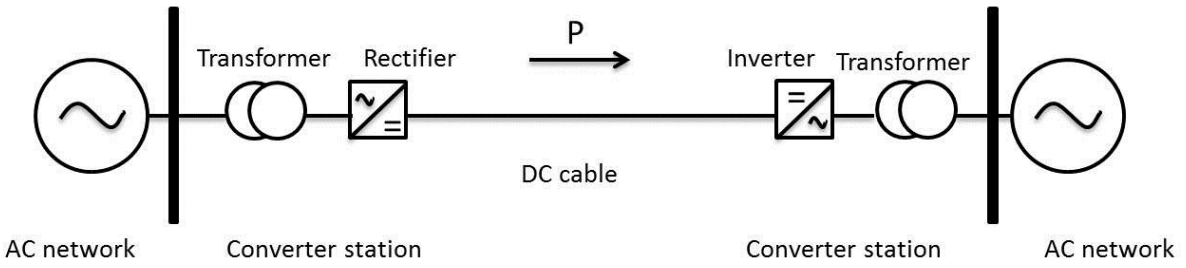

Figure 2.1. Basic HVDC topology.

Current Source Converter (CSC) technology, also called Line Commutated Converter (LCC) technology or HVDC classic, is a mature technology dating back to 1954 [3]. The technology is in use all over the world, interconnecting asynchronous AC systems, such as NORDEL and UCTE, and being used for long distance bulk power transfer. CSC HVDC uses semiconducting devices called thyristor valves to perform the conversion from AC to DC. Thyristors will only conduct when the anode voltage of the thyristor is higher than the cathode voltage [4]. This means that they rely on the external voltage of the AC network to operate. The converters also consume reactive power in both rectifier and inverter mode, which means external reactive power compensation, is needed. The main limitation of CSC HVDC is that it has to be supported by a strong AC network in both ends, making the current CSC technology unsuited for radial connections such as the connection of offshore wind farms and offshore petroleum industry.

Voltage Source Converter (VSC) HVDC was first introduced in 1997 and uses IGBTs, Insulated-Gate Bipolar Transistors, instead of thyristors [3]. IGBTs are self-commutating, which means they can be switched on and off regardless of the current flowing through them. As a result, VSC HVDC can be connected to weak AC systems, has no minimum power limit, and can provide black start capability. VSC HVDC can also control reactive power and due to advanced control methods, there is a significant reduction of harmonics. This means that VSC HVDC requires less AC filtering compared to CSC HVDC and also no reactive power compensation, reducing the size of the VSC HVDC converter. These factors make VSC HVDC the preferred solution for the connection of offshore wind farms. VSC HVDC does however experience slightly higher losses compared to CSC HVDC.

VSC HVDC converter stations use Pulse Width Modulation (PWM), the Multi-lever Converter, or a combination of the two [3]. A typical VSC converter station can be seen in figure 2.2 on the next page. The converter is connected to the grid through the AC transformer. The AC filter in combination with the phase reactors ensure the sinusoidal form of the AC voltage and reduce harmonics. The phase reactors also limit the short circuit currents and define the power flow between the AC and DC sides. The converter transforms the current from AC to DC, or vice versa. On the DC side, a DC capacitor is used to act as a low inductance path for the turned off converter current. It also contributes to harmonic filtering together with the DC reactors.

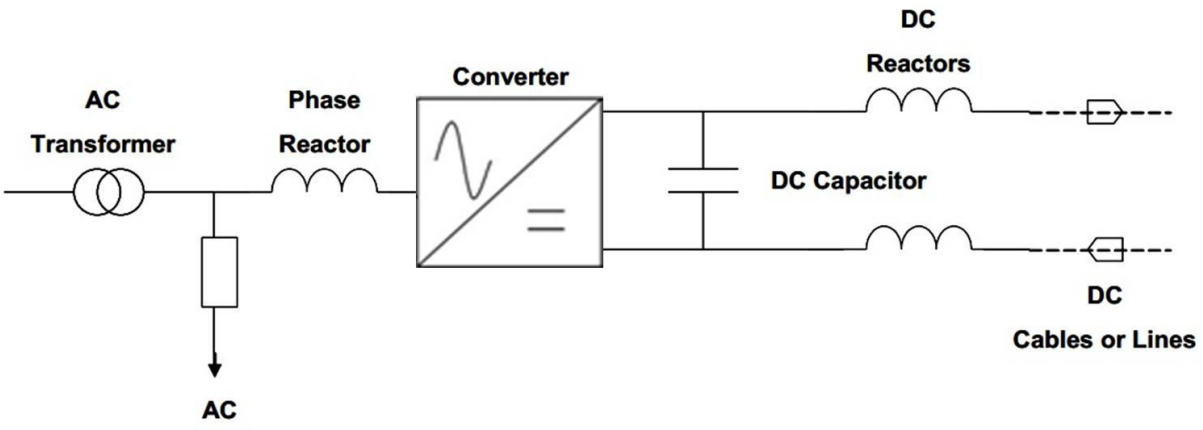

Figure 2.2. Diagram of a VSC HVDC system [3].

The resulting DC voltage from the VSC will contain transients originating from the switching of the power electronic components. The switching frequency can be in the kHz range, with the resulting harmonic frequencies a multiple of the switching frequency [5]. There is a 5 % total harmonic distortion (THD) limit for DC to AC conversion below 69 kV, while higher voltage levels have a THD limit of 2-3 % [6]. There is however no limit for harmonics occurring during AC to DC conversion. The THD can be lowered by installing filters, but this solution is limited by the offshore converter station's space and cost limitations. This means there is a significant risk of harmonics along offshore HVDC cables as a result of the rectifier and limited filtering.

High frequency harmonics will experience dampening along the HVDC cable length, meaning that the insulation closest to the rectifiers will experience the most severe harmonics [7]. This part of the cable also experiences the largest mechanical strain, and the cable connection is often designed to be quite flexible, facilitating the connection to the offshore converter station, and to some degree, reducing the mechanical strain on the cable. This does however also reduce the armoring of the cable connection, making this part of the cable more prone to water shielding fracture, which can lead to water intrusion, and as a result of the high frequency harmonics, facilitate water tree initiation and growth.

3. Electrical Water Treeing

Water treeing is a degradation mechanism creating structures in polymer insulation under the influence of humidity and AC stress. The phenomenon of water treeing was first discovered in the US during the late sixties, a few years after the introduction of extruded insulation such as cross-linked polyethylene (XLPE). XLPE was introduced as a replacement to paper insulation in medium voltage distribution cables. Water treeing drastically reduced the estimated lifetime of these new XLPE cables [8]. Consequently, studies on the water treeing phenomenon and the factors influencing the initiation and growth of water trees became, and still are, of great importance.

A water tree is a hydrophilic network within the insulation, consisting of strings of micro voids filled with water. Previous research has shown that the craze thickness in polyethylene is typically 0.1 - 0.5 µm [9]. Water trees are defined by four factors [10]. They are permanent. They have grown due to humidity and an electric field. They have a lower electrical strength when wet compared to the original polymer, but do not act as a local breakdown path or increase the probability for short circuit. Lastly, water trees are also more hydrophilic compared to the original polymer and typically have a much higher water content when wet. Water trees can facilitate the initiation of electrical trees, which in turn can lead to partial discharges and breakdown in the insulation.

3.1. Humidity in Polymers

Water can pass through organic materials, but not through metals and glass, due to the greater intermolecular spacing of the organic materials [11]. This means that water is likely to be absorbed and diffuse through polymeric materials such as XLPE insulation. Water has three different characteristic states in polymers. It can be distributed in between the polymeric chains as dissolved water, it can be bound to the surrounding polymers by intermolecular forces, and it can be found as liquid water, in the form of small enclosed droplets.

Henry's law can be used when considering diffusion through non-polar materials such as XLPE insulation and when considering dissolved water within the insulation itself [11]. Henry's law states that there is a linear relationship between the external vapor pressure and the corresponding water pressure within the polymer. The water content in polymeric materials will generally increase with increasing water temperature. This is a result of the higher vapor pressure that follows a higher temperature and the increased movement of the polymeric chains.

3.2. Types of Water Trees

Water trees are usually classified into two different types; vented water trees and bow-tie water trees [11]. Vented water trees are initiated on the interface between semiconductor and insulation, while bow-tie water trees are initiated from impurities within the insulation itself. Figure 3.1 shows the difference between a vented water tree and a bow-tie water tree.

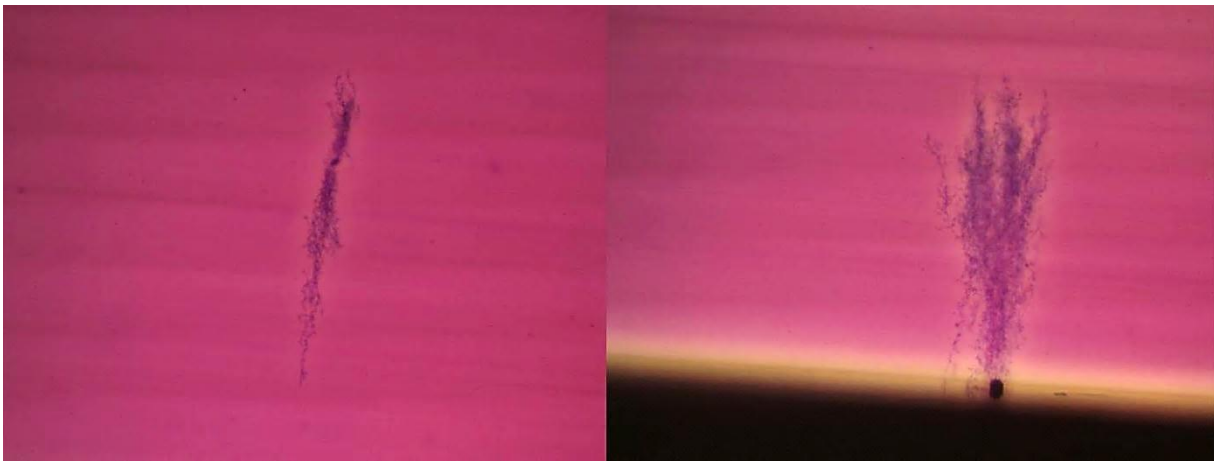

Figure 3.1. Picture of bow-tie water tree (left) and vented water tree (right).

Vented water trees are, as previously mentioned, initiated on the interface between the dielectric insulation and the semiconducting screen [11]. They grow symmetrically, in the same direction as the electrical field, towards the other side of the insulation, with water transported from the surroundings via the point of initiation. Impurities, mechanical damage and pollution on either the semiconducting screen or the insulation, are preferential sites for the initiation of vented water trees. Vented water trees can grow through the insulation, since they are subsequently filled with water transported from the root of the tree. This can lead to a breakdown in the insulation. As a result of this, vented water trees are usually considered more harmful than bow-tie water trees.

Bow-tie water trees are initiated from impurities or cavities within the dielectric insulation, with water dissolved from the surrounding insulation [11]. They grow symmetrically in the direction of the electric field, towards the two interfaces between the semiconducting screens and the dielectric insulation. Bow-tie water trees usually have a rapid initial growth, when the availability of dissolved water in the surrounding insulation is high, but this growth declines quickly, due to the limited humidity within the insulation. This reduces the total length of bow-tie water trees and such trees are rarely the reason for breakdown in XLPE insulated cables. Bow-tie water trees can however occasionally grow and connect with the interface between the semiconductor and the insulation, facilitating a vented water tree, and becoming a source of breakdown in the insulation. The difference in growth rate between a typical vented water tree and a typical bow-tie tree is illustrated in figure 3.2.

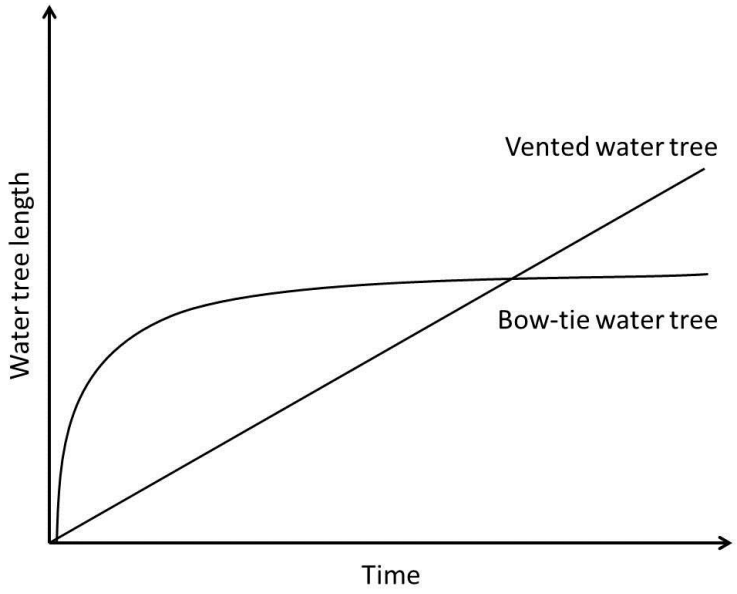

Figure 3.2. Typical growth rate for different water tree types [12].

3.3. Initiation and Growth

As previously mentioned, the two requirements for water tree initiation and growth is the application of an AC voltage and the presence of electrolyte (usually water) in contact with the polymer. A time lapse is often observed between the fulfillment of these conditions and the initiation of water tree growth [13]. This time lapse is called inception time. Inception time and water tree growth can be defined in terms of water tree length as a function of aging time as seen below in figure 3.3.

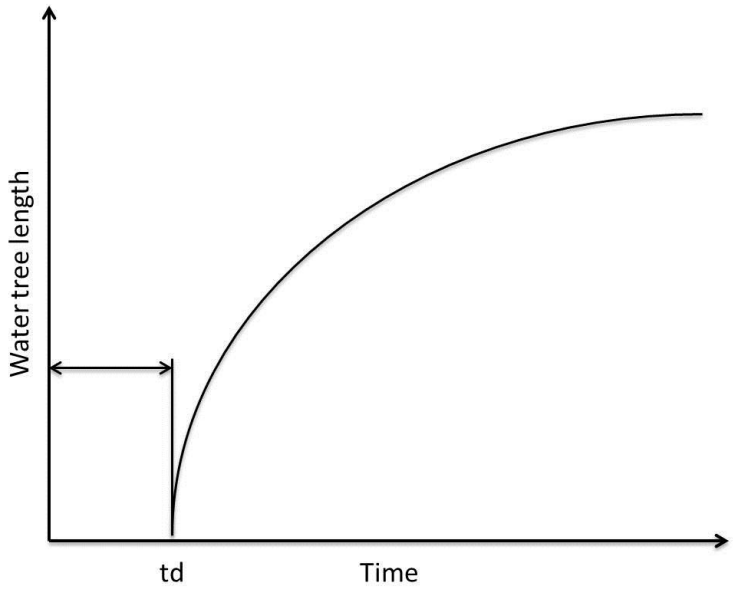

Figure 3.3. Empirical growth behavior of water trees showing the inception time, td [13].

Water trees grow in the direction of the electrical field. They can grow at electrical stress levels of less than 1 kV/mm and it is not possible to detect any partial discharges or emission of light during

initiation and growth. Factors affecting water tree growth are the availability of water, the degree of impurities, the type of polymer, the magnitude and frequency of the applied voltage, and the duration of ageing [13]. There are two main theories on the initiation and growth of water trees; the mechanical model and the electrochemical model [11]. However, due to the many factors and the complexity of the process, the basic mechanism for the initiation and growth of water trees is still under debate.

The mechanical model presumes that water tree initiation and growth is a result of localized mechanical over-stressing within the insulation [11]. Typical polyethylene insulation experiences large mechanical stress during extrusion and this can facilitate impurities within the insulation. With some degree of water saturation throughout the insulation, these impurities can experience a higher humidity compared to the rest of the insulation and as a result, higher Maxwell forces. These pulsating compressive Maxwell forces acting on enclosed water droplets within the insulation result in mechanical stress. Chain scission will occur if the resulting mechanical stresses exceed the local mechanical strength of the polymer. The result is crazing zones within the empty space. These zones can be filled with water due to diffusion and condensation from the surrounding insulation or the bottom of the tree. This will again result in higher Maxwell forces, and the water tree will keep on growing in the direction of the electrical field. External mechanical stress can in some cases increase the water tree growth. Figure 3.4 below shows the resulting Maxwell stresses of an electrical field and a water filled craze.

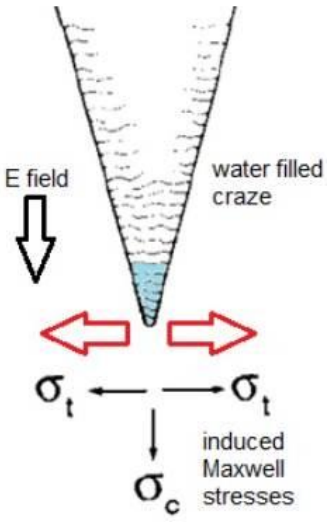

Figure 3.4. Sketch showing a mechanical model for initiation and growth of vented water trees [7].

The electrochemical model assumes that the growth of water trees is mainly a result of localized chemical reactions [11]. These reactions are strongly enhanced by the electric field and the availability of water, and will result in chain scission and the formation hydrophilic groups such as carboxylates at the interface between the polyethylene insulation and such an ion-conducting water tree. Hydrophilic groups have a tendency to interact and be dissolved by water and other polar substances, and will attract water within the insulation. Salts are one example of hydrophilic molecules. These hydrophilic groups form filamentary paths along the interface, causing enhanced diffusion and preferential sites for water condensation, facilitating further water tree growth.

The two different models do not necessary contradict each other and the general view is that water tree growth is a result of the two processes combined [11]. During chain scission caused by mechanical over stressing, radials are formed and these radials will initiate chemical reactions, thus contributing to the electrochemical growth of water trees. The result of chemical reactions might be reduced mechanical strength and thus lead to mechanical water tree growth. It is hard to distinguish between the primary and secondary effect, and most likely both of the mechanisms are involved, with the importance of each mechanism depending on the growth conditions.

Previous research has shown that the rate of water tree initiation and growth can be manipulated by changing the magnitude and/or frequency of the applied voltage [13]. It has been concluded that it is the resulting electric field and not the applied voltage that is the critical parameter. By increasing the applied voltage, and thus the applied electric field, the density of water trees and the length of water trees appear to increase. Figure 3.5 below shows the increase in the density of water trees relative to the applied electric field. The applied voltage was kept constant, while the applied electric field was manipulated by varying the insulation thickness.

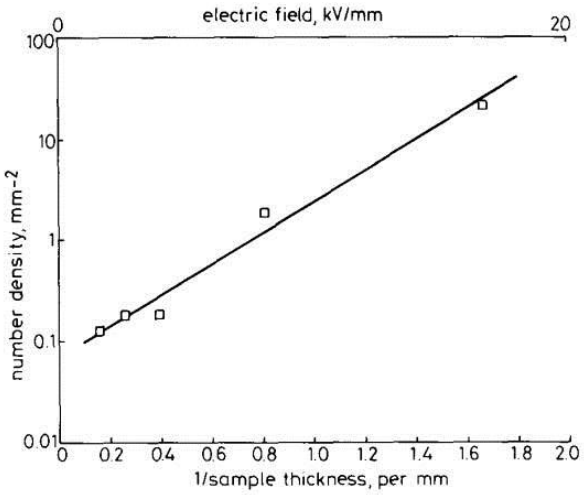

Figure 3.5. Number density of water trees as a result of varying applied electrical field. The applied voltage was kept constant, while the insulation thickness was varied. [13].

By varying the frequency of the applied voltage, previous research has concluded that the water tree density increases rapidly when the frequency varies between 600 Hz and 1.16 kHz [13]. This effect has not been fully understood, but it has been suggested that mechanical losses at this frequency may be significantly higher. The frequency also influences the water tree shape. A low frequency has been found to result in shorter and wider water trees, while a higher frequency has been found to result in longer and oblong water trees. Other factors such as impurities, the type of insulation and the availability of water also contribute to the rate of water tree initiation and growth, but have proven harder to quantify through research.

4. Methodology

This chapter describes the preparation of test objects, the laboratory setup and the experiments conducted.

4.1. Test Object Preparation

The laboratory experiments were performed on Rogowski shaped test objects. The test area of a Rogowski shaped test object is the bottom of the cup, which has an even electrical field distribution suitable for the experiments conducted in this master thesis. A finalized Rogowski test object ready for testing consisted of three components:

1) PE cup
2) Upper semiconductor
3) Lower semiconductor with a metal electrode

The three components were manufactured separately and then combined into a complete Rogowski shaped test object. There was a strict focus on cleanness during all parts of the manufacturing process as impurities lower the electrical properties of the insulation and had to be avoided at all costs. All equipment, tools and areas in contact with the material were cleaned thoroughly with isopropanol before use. A laminar air flow bench was used during all parts of the process to keep the particle pollution at a minimum. Components showing any visual irregularities or imperfections during the manufacturing process were discarded.

4.1.1. Extrusion

A standard AC polyethylene material capable of vulcanization was used as insulation. This material is used in XLPE insulated high voltage cables with voltages up to 300 kV [14]. The material was delivered as pellets and had to be extruded before being shaped into cups. Using extruded polyethylene, compared to pellets directly, reduced the chance of cavities and imperfections within the insulation.

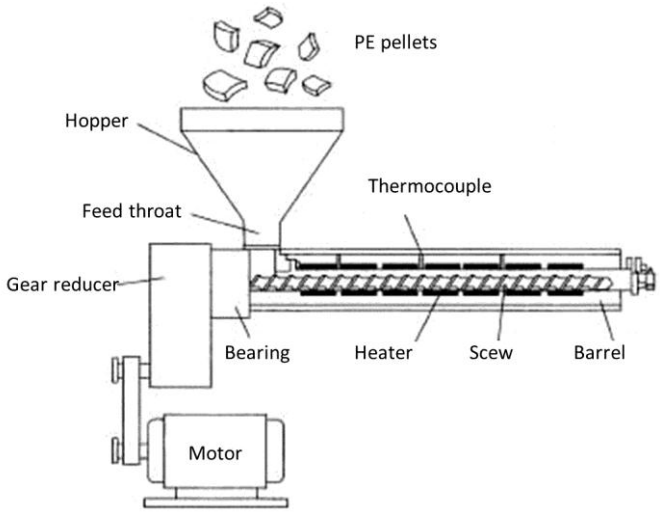

Figure 4.1. Basic extruder design, excluding extruder head [15].

Extrusion is an industrial production method used to process polyethylene during the manufacture of extruded cables. The principle of an extruder can be seen in figure 4.1. The material, which in this case was polyethylene pellets, is fed into the extruder through a funnel. A screw within the extruder transports the material through the barrel and the material is heated by the heating elements and the mechanical work that is carried out by the screw. The screw pitch changes along the barrel and this gradually increases the pressure on the material, kneading the material together and preventing cavities from emerging. At the end of the extruder, the material flows through an extruder head, shaping the material into a practical shape.

The extruder used in this master thesis had six different temperature zones and had to be dismantled and cleaned before use. The temperature settings for the six different zones can be seen in table 4-1 below. Zone 1 was located at the inlet funnel, while zone 6 was located just before the extruder head, at the end of the barrel. The speed of the screw within the extruder was set at 14 rotations per minute.

Table 4-1. Extruder temperature settings.

Zone	Temperature [°C]
1	117
2	117
3	117
4	117
5	117
6	15

A rectangular extruder head was used. This gave the final material a thick tape-form, which is ideal for the production of Rogowski type test objects. The material was run through a drum upon leaving the extruder head, cooling the material and making sure the material maintained its desired shape. The drum had to be run at a speed marginally higher than the speed of the screw. This kept the final shape of the material smooth, and prevented the formation of ripple. To reduce the chance of impurities within the insulation, the first 50 cm of extruded material was removed. The insulation tape was wrapped in aluminum foil after extrusion, before being heated to 80 °C in a heating cabinet. The wrapped and heated insulation tape was moved to a laminar air flow bench where the aluminum foil was removed and the tape was cut into smaller tablets, weighing about 28 grams each. The tablets were stored in a sealed box.

The extruder was cleaned after use. This was done using cleaning pellets. These pellets melt into liquid form, just like polyethylene, but the final material is much softer, and as a result, is much easier to remove. The extruder was then dismantled and thoroughly cleaned with a copper brush and isopropanol.

4.1.2. Casting of the PE Cup

Pre-shaped Rogowski cups were casted from the insulation tablets using casting molds and a hydraulic press. The molds were thoroughly cleaned with isopropanol before four layers of release agent (Frekote 55-NC) were applied. A five minute break was taken between each layer of release agent.

The optimal amount of insulation material in each mold was 31 grams and this meant that pellets had to be used in addition to the tablets. Since the tablets formed the bottom of the cups, while the pellets formed the upper part of the cup, the increased probability of cavities as a result of using pellets, should have little impact on the experimental results. Shims with a thickness of 1.5 mm were used to obtain an initial insulation thickness of 1.4 mm. The molds were covered in plastic sheeting to prevent surplus insulation material from adhering to the press during casting.

In this first phase of molding, the insulation material was only shaped and not vulcanized. This was done by keeping the temperature and the pressure of the hydraulic press within the limits given in table 4-2 below. The molds were dismantled after casting and the surplus material was removed using a scalpel. The pre-shaped Rogowski cups were placed in sealed plastic bags during storage.

Table 4-2. Hydraulic press settings for the casting of PE cups.

Process	Temperature[°C]	Pressure[tonnes]	Duration[minutes]
Low pressure	118	3.5	55
High pressure	118	25	12
Water cooling		25	18

4.1.3. Rolling of Semiconductor

A black cross-linking polyethylene material, compatible with the used XLPE insulation and specially designed for bonded semi conductive screen applications, was used for the manufacture of the upper and lower semiconductor. The material was supplied as pellets and was first dried in a vacuum chamber, at 60 °C, for a period of three days. This removed any humidity from the material. The material was then rolled, before being shaped into the upper and lower semi-conductor

The roller was located beneath a laminar air flow bench and had two roller elements with individual temperature control. The distance between the two roller elements was adjustable and this made it possible to wary the thickness of the semiconductor being produced.

The whole area was thoroughly cleaned with isopropanol before use. A copper knife was used to remove old pieces of semiconductor from the roller elements. The temperature of the front roller element and the back roller element were put at 105 °C and 115 °C respectively. During the heating of the roller elements, the distance between them was at a minimum. Pellets were then added between the two roller elements, before they were set to rotate. The distance between the two roller elements was gradually increased to 0.50 mm and the rolling continued until the semiconductor had acquired a smooth surface at that thickness. The temperature difference made the semiconductor adhere to the front roller element and the semiconductor was easily removed once the roller had cooled down, before being cut into smaller pieces, and placed in sealed plastic bags.

4.1.4. Upper Semiconductor

The casting molds used for the production of semiconductor were cleaned thoroughly with isopropanol before use. The molds had a diameter of 65 mm and a thickness of 0.5 mm. About 2.8 grams of semiconductor material was put in each of the casting molds. The casting molds were then covered with clean plastic sheeting to protect the semiconductor against impurities and placed in the hydraulic press. The settings of the hydraulic press can be seen in table 4-3.

Table 4-3. Hydraulic press settings for the casting of upper and lower semiconductor.

Process	Temperature[°C]	Pressure[tonnes]	Duration[minutes]
Low pressure	118	3.5	10
High pressure	118	25	2
Water cooling		25	8

The finished circular pieces of upper semiconductor were cut into pieces with a diameter of 54 mm and stored in sealed plastic bags.

4.1.5. Lower Semiconductor with Aluminum Electrode

The lower semiconductor was manufactured in the same way as the upper semiconductor. The only difference being an aluminum electrode, which was attached to the bottom of the semiconductor.

Aluminum foil with a thickness of 2 mm was cut into rectangles the size of 90x90 mm. One side of the foil was brushed with a steel brush. This increased the surface roughness and helped the semiconductor adhere better to the aluminum foil. The rectangular pieces of aluminum foil were then thoroughly washed in isopropanol and put on the top of the casting molds. The casting molds were placed in the hydraulic press and the machine was run with the same setting as for the upper semiconductor.

The surplus semiconductor material and aluminum foil was removed with a scissor after casting. The finished circular pieces of lower semiconductor had a diameter of 64 mm and were stored in sealed plastic bags.

4.1.6. Salt Particles

A 0.1 molar NaCl saline was produced from 0.5844 grams of NaCl and 0.1 liter of demineralized water. 20 salt particles were applied on the surface of each lower semiconductor. Salt particles are hydrophilic and can attract water within the insulation, increasing the regional humidity and thus facilitate water tree initiation and growth. All salt particles were applied in the region of homogenous field distribution using a syringe with 0.5 µl capacity. Each droplet was approximated with 0.1 µl of the NaCl saline. The droplets were then dried using a vacuum chamber at 60 °C for thirty minutes.

4.1.7. Vulcanization (cross-linking)

Vulcanization is a chemical process that converts polymers into more durable materials by forming cross-links between the individual polymer chains [14]. Polyethylene can be cross-linked using heat and high pressure, causing the material to go through a curing process, preventing future reshaping. Cross-linked polyethylene, commonly abbreviated XLPE or PEX, has higher thermal resistance, increased tensile and impact strength, higher scratch resistance and is less prone to brittle fracture. The chemical resistance of the material is also enhanced. This means that XLPE-insulation can handle higher current densities and operational temperatures compared to PE-insulation. XLPE-insulation can be operated at a temperature of 125 °C and can sustain short fault-temperatures of 250 °C [11].

The PE cup, the upper semiconductor and the lower semiconductor were combined into a complete Rogowski shaped test object using vulcanization. The PE cups, with the upper and lower semiconductor, were vulcanized in the same casting molds they were casted in, making it easier to dismantle the casting molds after vulcanization. Shims with a thickness of 0.45 mm were added on

top of the casting molds. This gave the finished test objects an insulation thickness of 1.1 mm. A plastic film was placed on top of the casting molds to prevent excess insulation material from adhering to the hydraulic press. The hydraulic press was run with the settings given in table 4-4 below. The high temperature and pressure resulted in vulcanization. Surplus insulation material was removed with a scalpel after vulcanization.

Table 4-4. Hydraulic press settings for vulcanization.

Process	Temperature[°C]	Pressure[tonnes]	Duration[minutes]
Low pressure	170	3.5	1
High pressure	170	25	45
Water cooling		25	18

4.1.8. Relaxation and Degassing

Mechanical relaxation was performed to improve the mechanical properties of the XLPE-insulation. This was done by placing the vulcanized Roowski shaped test objects in a ventilated heating cabinet at 130 °C. The relaxation process removed some of the mechanical stress acquired by the test objects during vulcanization. The heat was turned down to 90 °C once the XLPE-insulation turned transparent. The test objects were then kept in the heating cabinet at this temperature for three days. This last process is called degassing and removed volatile byproducts from the vulcanization process [14].

4.1.9. Preconditioning with Demineralized Water

The test objects were preconditioned with demineralized water before testing. This was done to saturate the XLPE insulation with water and to facilitate the initiation of water trees. The test objects were filled with demineralized water and then sealed off using a XLPE cover. Evaporation of water was prevented by sealing the lid with silicone. The test objects were left in a heating cabinet at 30 °C for four weeks to ensure saturation all the way through the XLPE insulation. Figure 4.2 below presents a complete Rogowski shaped test object ready for ageing.

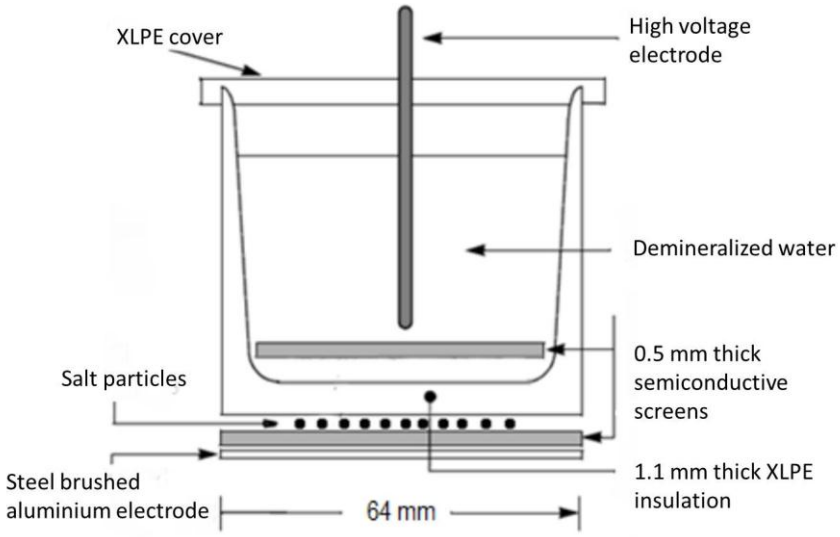

Figure 4.2. Complete Rogowski shaped test object ready for testing [16].

4.2. Experimental Setup

An experimental setup capable of applying a DC voltage with a superimposed high frequency AC component was used to simulate the HVDC component and the overlaying transients that occur close to the power electronics used for HVDC converters. The experimental setup used in this master thesis was developed by Petter I. Nodeland [17] and further improved by Martin Amundsen [18]. Figure 4.3 presents a principal sketch of the experimental setup.

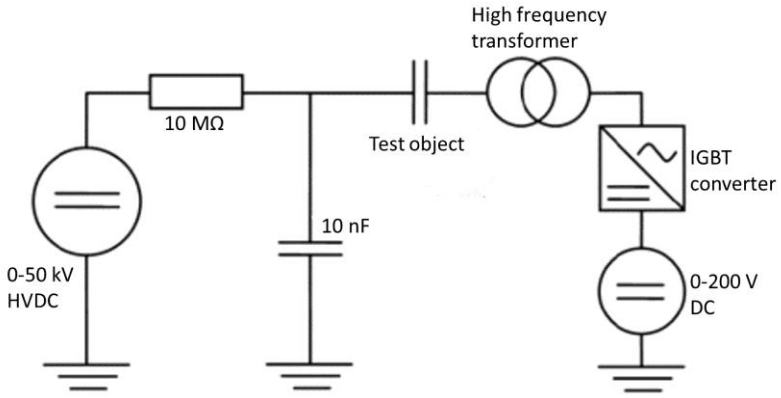

Figure 4.3. Principal sketch of the experimental set-up. The test object can be supplied with DC from the HVDC source on the left side and/or a high frequency AC component through a high frequency transformer supplied from an IGBT converter on the right side [16].

As seen in figure 4.3 above, the test object is represented by a capacitance. The left side of the test object is connected to a 50 kV Spellman DC voltage source. The voltage source is protected by a 10 MΩ short circuit resistance in case of test object breakdown. On the other side of the test object a 0-200 V DC source supplies an IGBT converter. The IGBT converter has its frequency and amplitude controlled by a signal generator and is connected to the test object through a high frequency controller. This allows the application of a variable high frequency AC voltage across the test object. A 10 nF capacitor is located on the DC side of the test object to create a path for the AC current. A complete figure of the electrical circuit and in-depth explanations regarding the experimental setup and the individual components can be found in [17].

Further security measures have been taken to protect the components in the electrical circuit. A sphere gap has been placed in parallel with the high frequency transformer to protect the transformer against high voltages in the event of breakdown. A gas sphere gap has been placed on the primary side of the transformer as further protection. The DC voltage and current was measured at the sphere gaps on the high voltage side of the high frequency transformer. The software LabVIEW was used to supervise the magnitude of this voltage and current. A voltage drop at the DC source and/or a rapid increase of current through the IGBT, which both can occur during breakdown, would result in a disconnection of the voltage sources.

The test objects were located in a heating cabinet at all times during testing. The temperature was set at 30 °C and kept constant during testing. The AC-voltage was imposed on the lower semi-conductor, while the DC-voltage was imposed on the upper semi-conductor through a metal electrode. Two different rounds of experiments were conducted. The first set of experiments was conducted using the high frequency AC component only, while the second round of experiments combined the same high frequency AC component, with a superimposed DC component. For both

sets of experiments, nine Rogowski style test objects were aged. Three test objects were removed after one week of ageing, another three after two weeks of ageing, and the final three test objects were removed after three weeks of ageing.

4.2.1. High Frequency AC Component

Experiments were first conducted with the high frequency AC component as the only voltage imposed across the test objects. The peak to peak magnitude of the high frequency AC component was calculated by keeping the resulting electrical field strength in the insulation equal to experiments previously conducted on the same topic [12]. The calculation can be seen in equation 4.1 below.

$$V_{AC} = E_{AC} \times d = 2.05 \times 2\ \frac{kV}{mm} \times 1.1\ mm = 4.51\ kV \qquad (4.1)$$

The frequency of the signal generator was set at 15 kHz and the voltage amplitude was set at 5 V. The DC source feeding the AC-side was then increased until a resulting high frequent AC voltage with a magnitude of 4.51 kV was obtained. The 15 kHz frequency is higher than the frequency which can be expected in real transmission networks [19], but has been chosen as it is within the optimal frequency range of the transformer. The resulting AC stress can be seen below in figure 4.4.

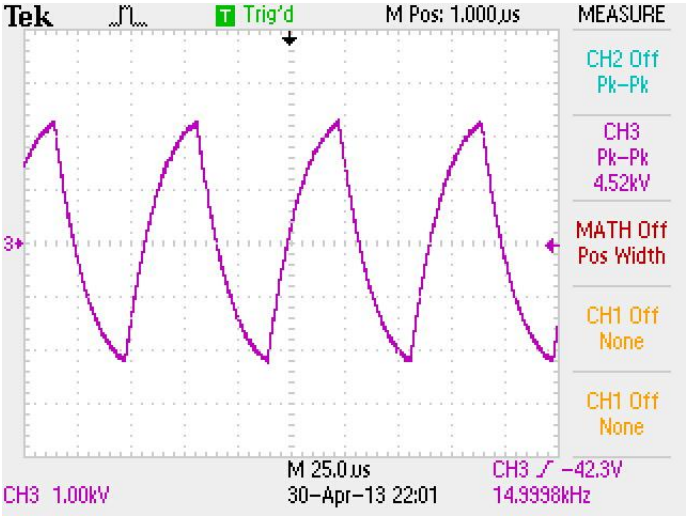

Figure 4.4. Resulting AC stress on the high voltage side of the high frequency transformer.

As seen in figure 4.4, the resulting AC stress was of a triangular shape with a frequency of 15 kHz. A Fast Fourier Transform was performed with the oscilloscope to find the harmonics. Figure 4.5 on the next page illustrates how the AC voltage contained a significant share of harmonics with different frequencies, all a multiple of 15 kHz.

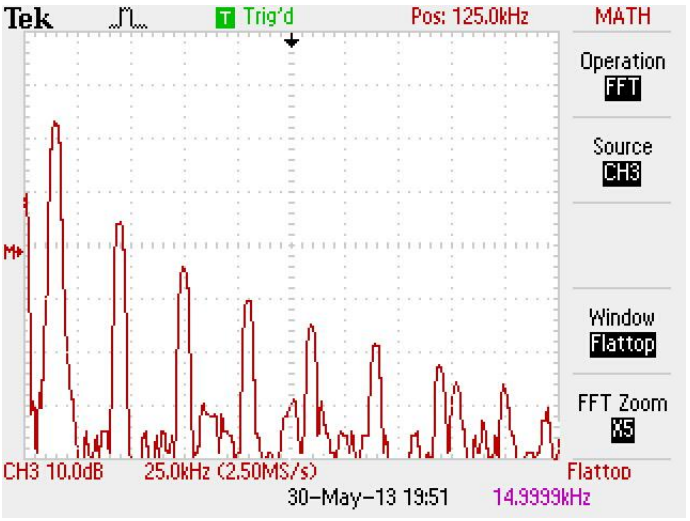

Figure 4.5. The different frequency components of the high frequency AC component.

4.2.2. DC Voltage with Superimposed High Frequency AC Component

A new set of experiments were conducted, but this time with a DC voltage imposed across the test objects in addition the high frequency AC component. The DC source was turned on before the AC source. The voltage of the DC component was set at 13,2 kV, while the AC component had the same peak to peak value as in the previous set of experiments, corresponding to a ripple of 17.1 %. The resulting electrical field strength of the DC component is calculated in equation 4.2 below.

$$E_{DC} = \frac{U}{d} = \frac{13.2\ kV}{1.1} = 12kV/mm \qquad (4.2)$$

4.3. Water Tree Analysis

All the Rogowski shaped test objects were disassembled after testing. The bottom part, consisting of the two semiconductors and the insulation, was sliced into 0.5 mm thick cuts using a microtron. Sixty cuts were taken from each test object, ensuring that the area being investigated had been exposed to a homogenous electrical field. The cuts were dyed with methylene blue using the CIGRE standard methylene blue procedure. The ingredients were mixed in a glass container using a magnetic stirrer and the mixing ratio shown below in table 4-5.

Table 4-5. Mixing ratio for CIGRE standard methylene blue procedure.

Ingredient	Amount
Methylene blue	54 g
Sodium carbonate (Na_2CO_3)	4,5 g
Tap water	1,8 l

The container was then covered with aluminum foil to reduce evaporation and put in a heating cabinet at 67.5 °C. The mixing and dyeing procedure can be seen in table 4-6.

Table 4-6. Procedure for the mixing of methylene blue and the dyeing of insulation cuts.

Process	Time [h]
Magnetic stirrer on	5
Magnetic stirrer off	20
Magnetic stirrer on	1.5
Magnetic stirrer off and cuts placed in methylene blue mixture for dyeing	4.5

The cuts were removed from the container after dyeing, rinsed with water, and placed in a glass container with warm water for a day. This last process improved the coloring of the water trees.

All cuts were investigated with an optical microscope at 25-50 times of magnification. All water trees were photographed and measured using the software ZEN 2011. Cuts containing water trees were then put aside, with the type of water tree and the length of the water tree being noted. The initiation location was also noted down in the case of vented water trees (upper or lower semiconductor).

5. Results

Two sets of experiments were conducted in this master thesis. The first set of experiments was conducted using a high frequency AC component only, while the second set of experiments was conducted using a DC voltage with a superimposed high frequency AC component. All test objects experienced significant water tree initiation and growth. The water tree analysis found vented water trees, initiated at both the upper and lower semiconductor, and bow-tie water trees, in both sets of experiments.

5.1. High Frequency AC Component

All test objects exposed to a high frequency AC component experienced water tree initiation and growth. The water trees were quite evenly distributed among the different test objects. Tables showing the water trees observed in each individual test object can be found in appendix A.

5.1.1. Development of the Longest Water Tree

The longest observed water tree after one week of ageing was a bow-tie water tree with a length of 471 µm. This corresponded to 43 % of the total insulation thickness. The water tree is presented in figure 5.1 below.

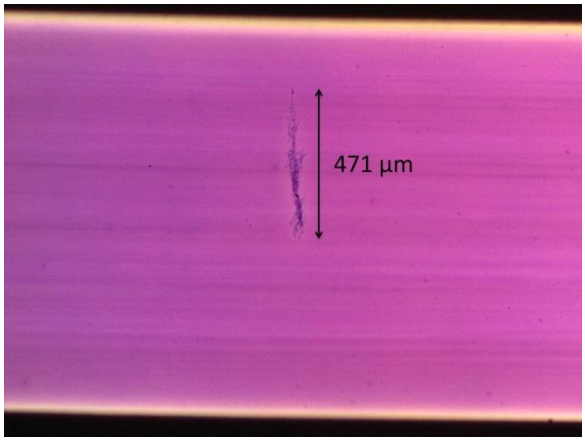

Figure 5.1. Longest observed water tree after one week of ageing exposed to a high frequency AC component only.

After two weeks of ageing, the longest observed water tree was a vented water tree from the upper semiconductor, and at 477 µm, only slightly longer than the one observed after one week of ageing. This length corresponded to 43 % of the total insulation thickness. The water tree is shown in figure 5.2.

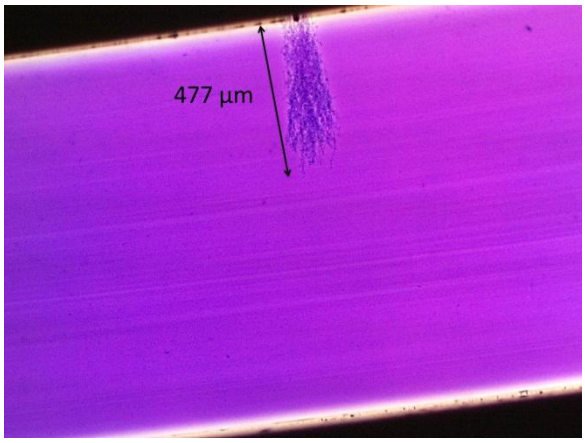

Figure 5.2. Longest observed water tree after two weeks of ageing exposed to a high frequency AC component only.

After three weeks of ageing, the longest observed water tree was a bow tie water tree with a length of 607 µm, corresponding to 55 % of the total insulation thickness. The water tree is presented below in figure 5.3.

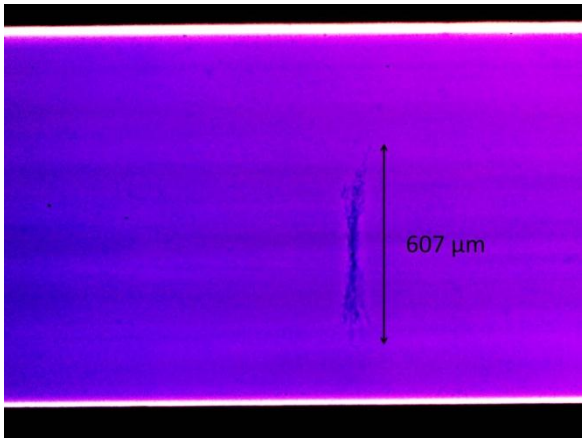

Figure 5.3. Longest observed water tree after three weeks of ageing exposed to a high frequency AC component only.

There was only a slight increase in the length of the longest observed water tree from week to week. Two of the three water trees were bow-tie water trees, but it should be noted that many of the vented water trees that were observed in the insulation were of almost comparable length to these bow-tie water trees. Figure 5.4 depicts the development of the longest observed water tree as a function of the ageing duration.

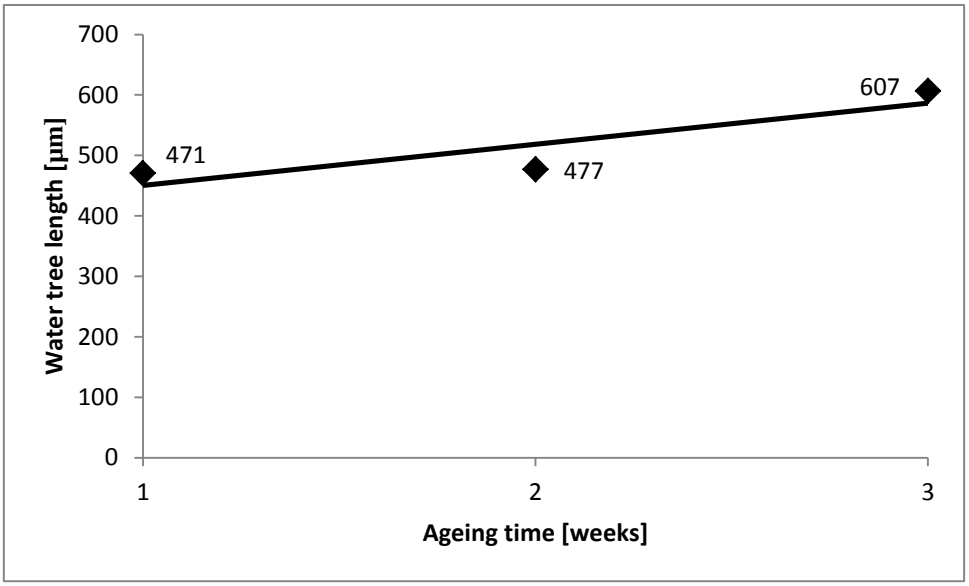

Figure 5.4. Longest observed water tree as a function of time. Test objects were exposed to a high frequency AC component only.

5.1.2. Bow-tie Water Trees

Bow-tie water trees were observed in all but one test object. 7 bow-tie water trees were observed after one week of ageing. After two weeks of ageing, 22 bow-tie water trees were observed. After three weeks of ageing, the number had increased even further and 53 bow-tie water trees were observed in the three test objects. Figure 5.5 below illustrates the increase in observed bow-tie water trees as a function of ageing time.

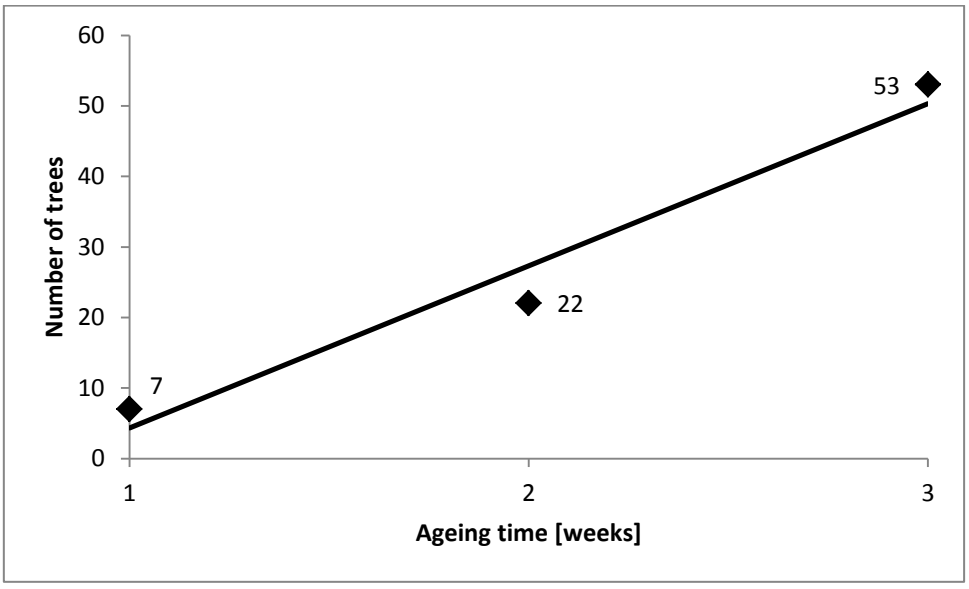

Figure 5.5. Number of observed bow-tie water trees as a function of time. Test objects were exposed to a high frequency AC component only.

As seen in table 5-1, the average length of the observed bow-tie water trees was lower after two and three weeks of ageing, compared to one week of ageing, while the relative standard deviation increased.

Table 5-1. The average length and standard deviation of the observed bow-tie water trees. Test objects were exposed to a high frequency AC component only.

Ageing time [weeks]	Average length [µm]	Standard deviation [µm]
1	333.9	124.3
2	245.6	96.7
3	275.5	128.0

5.1.3. Vented Water Trees from Upper Semiconductor

Vented water trees from the upper semiconductor were observed in all test objects. After one week of ageing, 21 vented water trees were observed from the upper semiconductor. The number increased to 34 after two weeks of ageing. In the last three test objects, which had aged for three weeks, a total of 26 vented water trees from the upper semiconductor were observed. Figure 5.6 below depicts the number of observed vented water trees from the upper semiconductor as a function of the ageing duration.

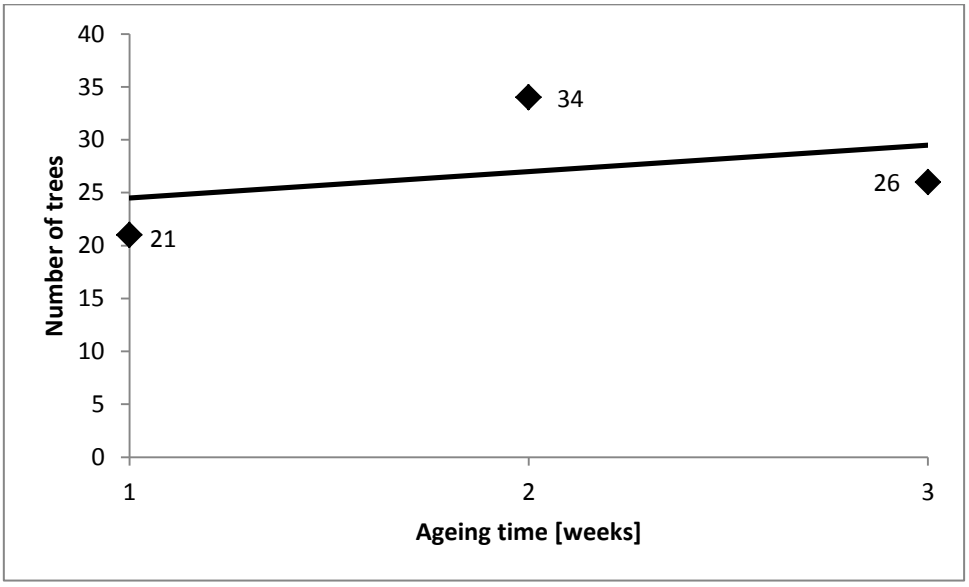

Figure 5.6. Number of observed vented water trees from the upper semiconductor as a function of time. Test objects were exposed to a high frequency AC component only.

The average length of the vented water trees from the lower semiconductor increased slightly between two and three weeks of ageing, while the standard deviation remained stable. Table 5-2 presents the average length and the corresponding standard deviation for vented water trees at the lower semiconductor.

Table 5-2. The average length and standard deviation of the observed vented water trees from the upper semiconductor. Test objects were exposed to a high frequency AC component only.

Ageing time [weeks]	Average length [µm]	Standard deviation [µm]
1	301.2	90.2
2	295.3	90.0
3	337.0	94.3

5.1.4. Vented Water Trees from Lower Semiconductor

Only one vented water tree was observed at the lower semiconductor after one week of ageing. 6 vented water trees were observed at the lower semiconductor after two weeks of ageing. After three weeks of ageing, the number of vented water trees observed at the lower semiconductor had drastically increased to 35. Figure 5.7 below illustrates the almost exponential increase in vented water trees from the lower semiconductor as a function of ageing time.

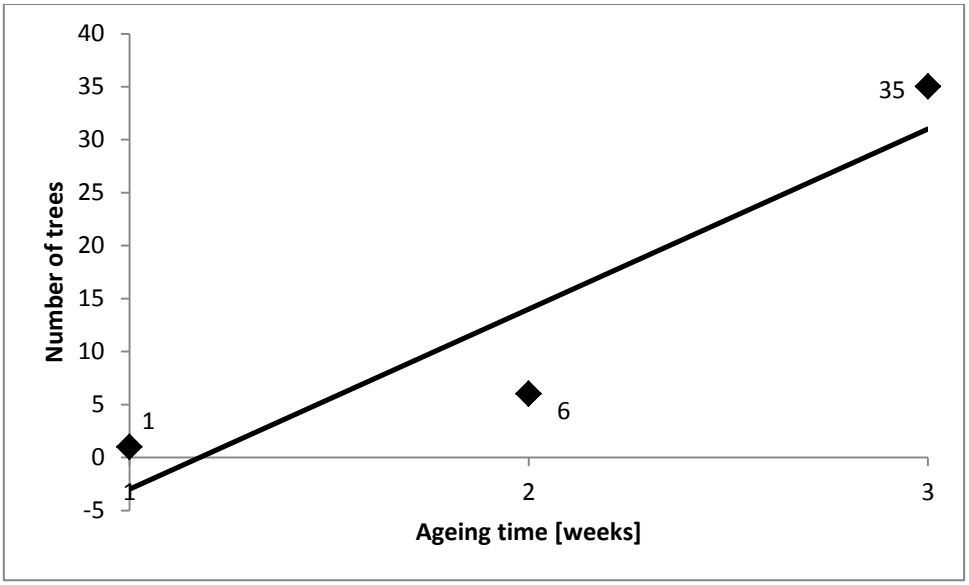

Figure 5.7. Number of observed vented water trees from the lower semiconductor as a function of time. Test objects were exposed to a high frequency AC component only.

The average length of the observed vented water trees from the lower semiconductor increased with the ageing time and can be seen in table 5-3 below. The standard deviation declined between two and three weeks of ageing, but remained large relative to the average length.

Table 5-3. The average length and standard deviation of the observed vented water trees from the lower semiconductor. Test objects were exposed to a high frequency AC component only.

Ageing time [weeks]	Average length [µm]	Standard deviation [µm]
1	64	-
2	120.3	91.3
3	170.9	74.8

5.1.5. Aggregated Water Tree Density and Average Water Tree Length

The aggregated water tree density was acquired by combining the number of observed bow-tie water trees with the number of observed vented water trees from both the upper and the lower semiconductor. After one week of ageing, the total number of observed water trees was 29. The density of observed water trees increased drastically with the ageing time. Another week of ageing increased the number to 62, while three weeks of ageing resulted in 114 observed water trees. Figure 5.8 depicts the trend in aggregated water tree density as a function of the duration of ageing.

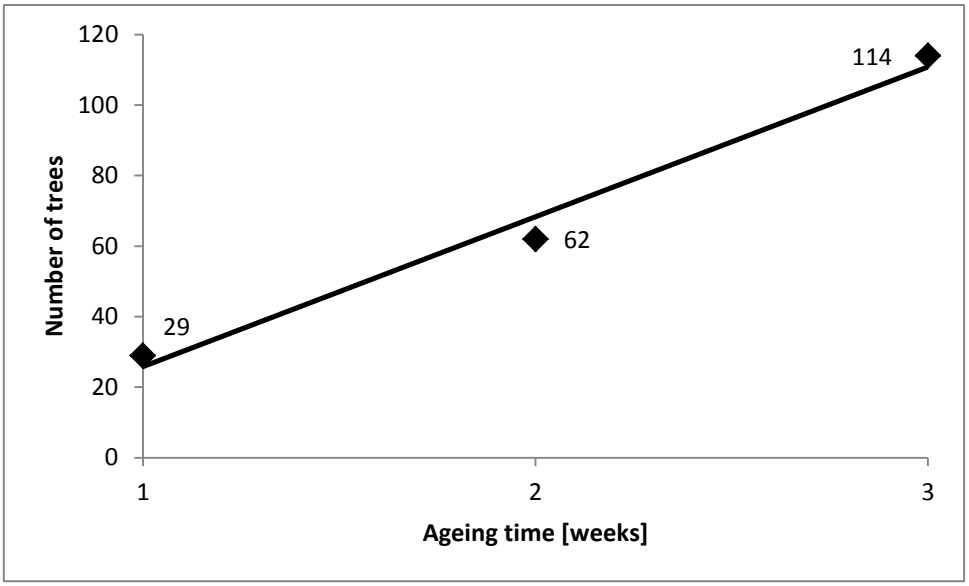

Figure 5.8. Aggregated number of observed vented and bow-tie water trees as a function of time. Test objects were exposed to a high frequency AC component only.

The average aggregated water tree length declined as the ageing duration increased. After one week of ageing the average water tree length was 300.9 µm, with a standard deviation of 106.7 µm. Two weeks of ageing resulted in an average aggregated water tree length of 260.8 µm, with a standard deviation of 104.7 µm. After three weeks of ageing, the resulting aggregated water tree length was 257.4 µm, with a standard deviation of 122.9 µm. The average aggregated water tree length as a function of ageing duration can be seen in figure 5.9 below.

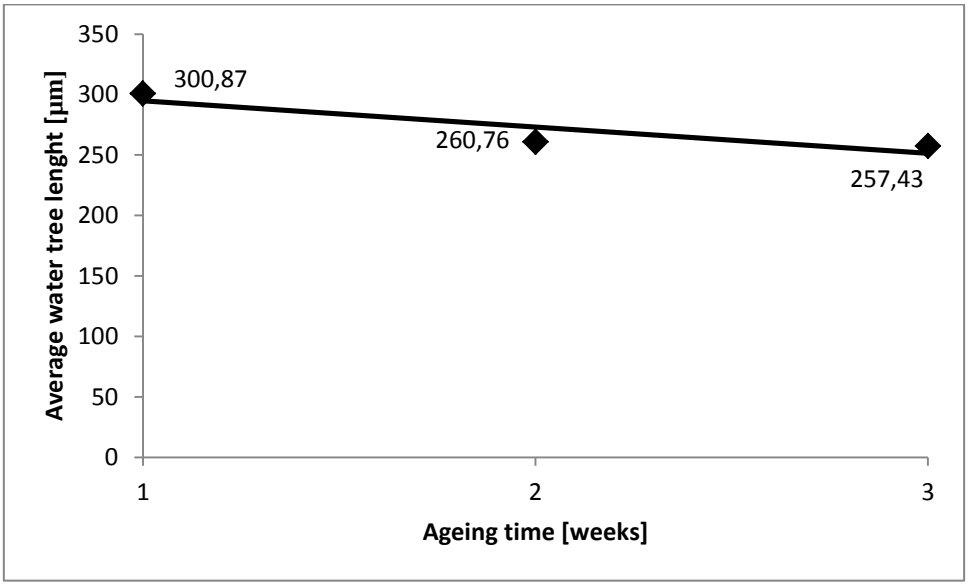

Figure 5.9. Average aggregated water tree length as a function of time. Test objects were exposed to a high frequency AC component only.

5.2. DC Voltage with Superimposed High Frequency AC Component

All test objects exposed to a DC voltage with a superimposed high frequency AC component experienced water tree initiation and growth. Some variations in water tree density were observed for test objects subjected to the same duration of ageing. Tables showing the water trees observed in

each individual test object can be found in appendix B. Two out of three test objects experienced breakdown before enduring three complete weeks of ageing. It has been assumed that the breakdown was caused by water trees bridging the insulation, as this seems the only plausible explanation. The results from the only test object to experience three complete weeks of ageing has been multiplied with 3 to make linear regression possible. This is a crude simplification and has to be kept in mind when assessing the graphs. The data could also have been presented as the number of water trees per cut, or water trees per test object, but none of these approaches would have improved the statistical credibility.

5.2.1. Development of the Longest Water Tree

The longest observed water tree after one week of ageing was a vented water tree from the lower semiconductor. The water tree was 528 µm long, corresponding to 48 % of the total insulation thickness, as shown in figure 5.10 below.

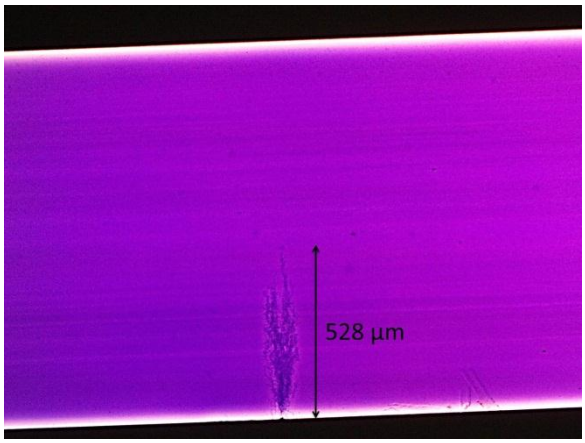

Figure 5.10. Longest observed water tree after one week of ageing exposed to a DC voltage with a superimposed high frequency AC component.

After two weeks of ageing, the longest observed water tree was a vented water tree from the upper semiconductor. The water tree was 476 µm long, corresponding to 43 % of the total insulation thickness. The water tree is presented in figure 5.11 below.

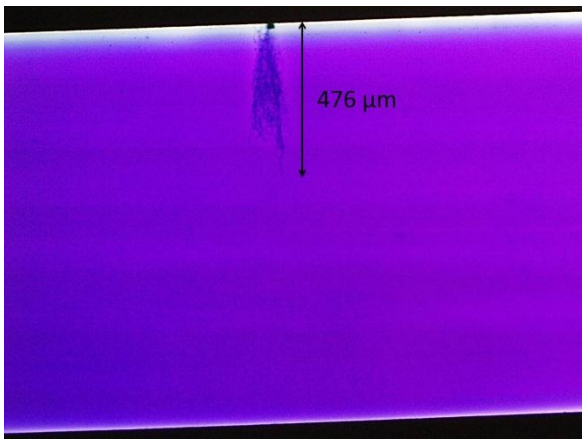

Figure 5.11. Longest observed water tree after two weeks of ageing exposed to a DC voltage with a superimposed high frequency AC component.

Two out of three test objects experienced breakdown before completing three weeks of ageing. This was most likely a result of a water trees bridging the insulation. Hence, the longest water tree before three weeks of ageing can be said to have been 1100 µm, corresponding to 100 % of the total insulation thickness. The first breakdown occurred after two weeks and 52 hours of ageing and is shown below in figure 5.12. The second breakdown occurred after two weeks and 55 hours of ageing.

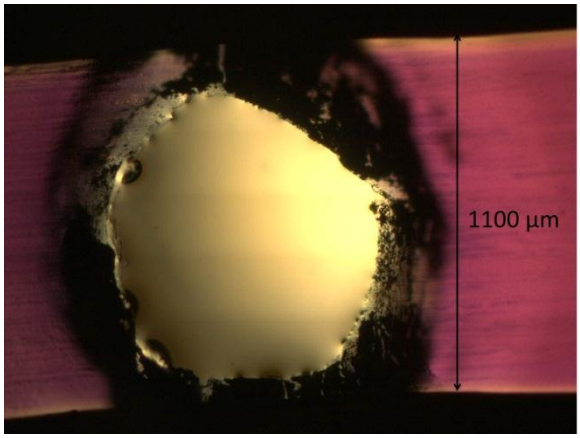

Figure 5.12. Breakdown observed after two weeks and 52 hours of ageing exposed to a DC voltage with a superimposed high frequency AC component.

There was a slight reduction in the length of the longest observed water tree between one and two weeks of ageing. However, after three weeks of ageing, the longest water tree bridged the insulation and caused a breakdown. Figure 5.13 below depicts the development of the longest observed water tree as a function of ageing time.

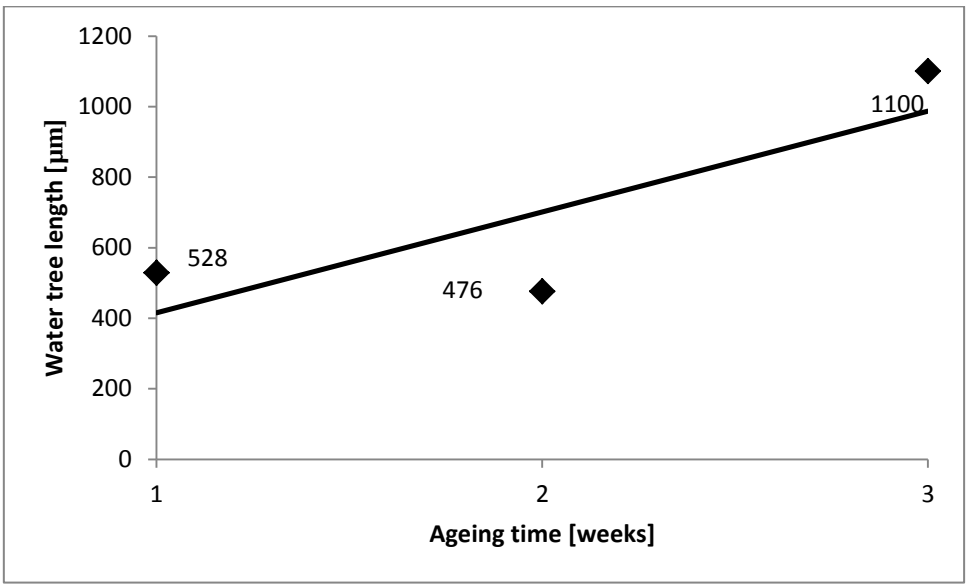

Figure 5.13. Longest observed water tree as a function of time. Test objects were exposed to a DC voltage with a superimposed high frequency AC component.

5.2.2. Bow-tie Water Trees

Bow-tie water trees were observed in all test objects. 8 bow-tie water trees were observed after one week of ageing. After two weeks of ageing, the number of observed bow-tie water trees had

increased to 11. After three weeks of ageing, 11 bow-tie water trees were observed in the one test object that completed three whole weeks of ageing. Figure 5.14 illustrates the increase in the number of observed bow-tie water trees as a function of ageing time. The number of observed bow-tie water trees in the only test objects to complete three weeks of ageing has in this figure been multiplied by 3.

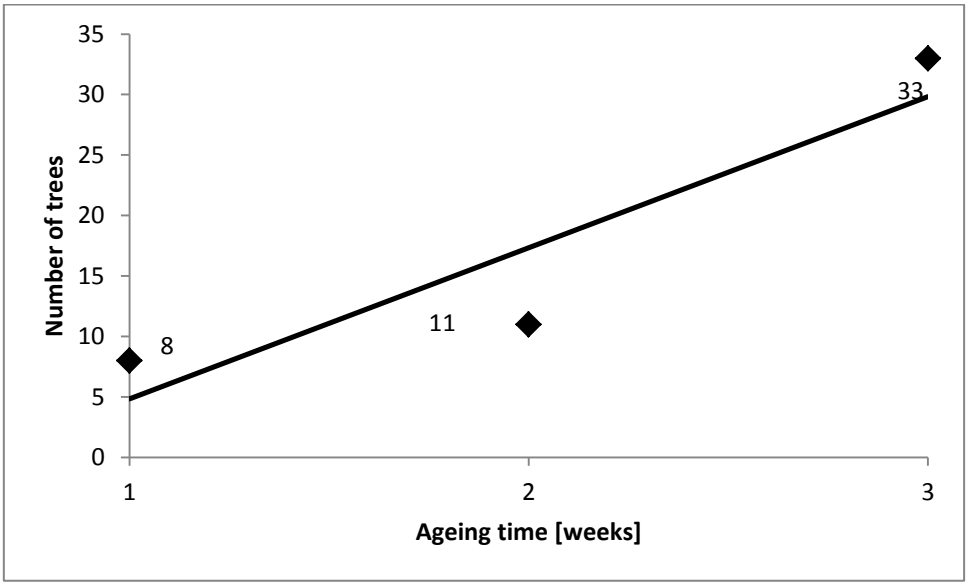

Figure 5.14. Number of observed bow-tie water trees as a function of time. Test objects were exposed to a DC voltage with a superimposed high frequency AC component.

The average length and the corresponding standard deviation for the bow-tie water trees observed in the insulation can be seen below in table 5-4. There was a drastic increase in the standard deviation between two and three weeks of ageing.

Table 5-4. The average length and standard deviation of the observed bow-tie water trees. Test objects were exposed to a DC voltage with a superimposed high frequency AC component.

Ageing time [weeks]	Average length [µm]	Standard deviation [µm]
1	396.9	136.1
2	211.1	65.1
3	290.3	140.7

5.2.3. Vented Water Trees from Upper Semiconductor

Vented water trees from the upper semiconductor were observed in all test objects. 8 vented water trees were observed from the upper semiconductor after one week of ageing. After two weeks of ageing, 18 vented water trees were observed from the upper semiconductor. 8 vented water trees were observed from the upper semiconductor in the single test object that completed three weeks of ageing. Figure 5.15 illustrates the number of observed vented water trees from the upper semiconductor as a function of ageing time. The number of observed vented water trees from the upper semiconductor in the only test object to complete three weeks of ageing has in this figure been multiplied by 3.

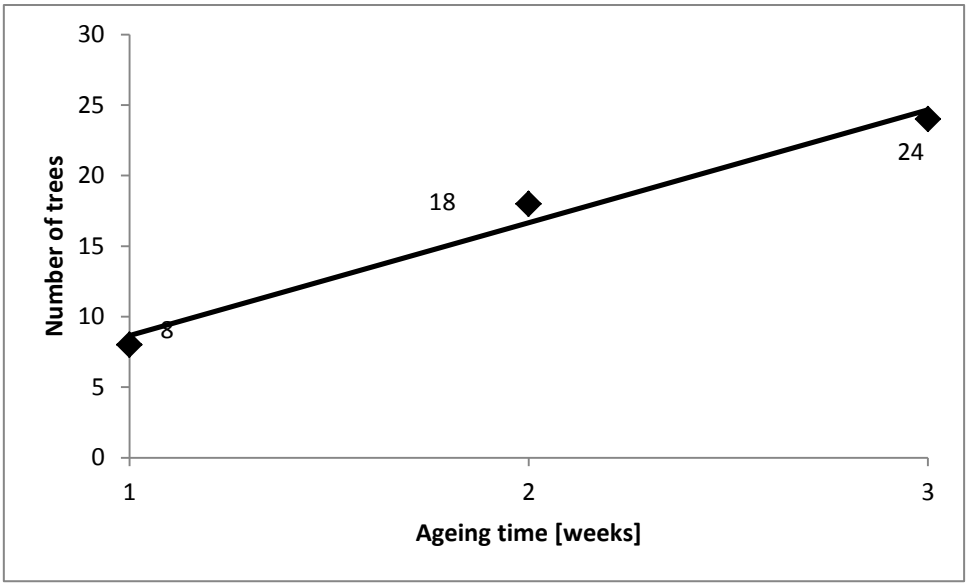

Figure 5.15. Number of observed vented water trees from the upper semiconductor as a function of time. Test objects were exposed to a DC voltage with a superimposed high frequency AC component.

The average length and the corresponding standard deviation for the vented water trees observed from the upper semiconductor can be seen in table 5-5 below. There was a drastic increase in the standard deviation between two and three weeks of ageing.

Table 5-5. The average length and standard deviation of the observed vented water trees from the upper semiconductor. Test objects were exposed to DC voltage with a superimposed high frequency AC component.

Ageing time [weeks]	Average length [µm]	Standard deviation [µm]
1	331.4	89.4
2	326.7	85.6
3	253.3	125.7

5.2.4. Vented Water Trees from Lower Semiconductor

Numerous vented water trees from the lower semiconductor were observed in all test objects. After one week of ageing, a total of 23 vented water trees were observed from the lower semiconductor. 13 of the vented water trees were observed in one test object, while the two other test objects experienced 5 each. 64 vented water trees were observed from the lower semiconductor after two weeks of ageing. Only 13 vented water trees were observed from the lower semiconductor in the single test object that completed three weeks of ageing. Figure 5.16 presents the number of vented water trees observed from the lower semiconductor as a function of ageing time. The number of vented water trees from the lower semiconductor in the only test object to complete three weeks of ageing has in this figure been multiplied by 3.

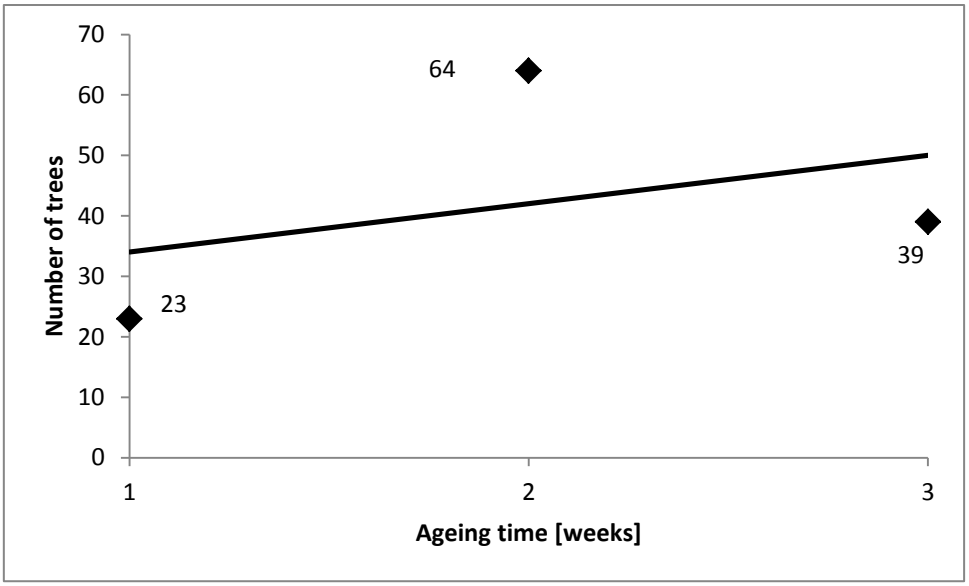

Figure 5.16. Number of observed vented water trees from the lower semiconductor as a function of time. Test objects were exposed to a DC voltage with a superimposed high frequency AC component.

As seen in table 5-6 below, the average length of the observed vented water trees from the lower semiconductor increased with the increasing duration of ageing. The standard deviation increased drastically between two and three weeks of ageing.

Table 5-6. The average length and standard deviation of the observed vented water trees from the lower semiconductor. Test objects were exposed to a DC voltage with a superimposed high frequency AC component.

Ageing time [weeks]	Average length [µm]	Standard deviation [µm]
1	170.6	87.4
2	206.7	81.4
3	300.6	152.3

5.2.5. Aggregated Water Tree Density and Average Water Tree Length

The aggregated water tree density was acquired by combining the number of observed bow-tie water trees with the number of observed vented water trees from both the upper and the lower semiconductor. After one week of ageing, a total of 39 water trees were observed in the insulation. A significant increase was observed between one and two weeks of ageing, and a total of 93 water trees were observed after two weeks of ageing. A total of 33 water trees were observed in the only test object to complete three weeks of ageing. Figure 5.17 depicts the increase in the aggregated number of observed water trees as a function of ageing time. The number of observed water trees in the single test object to complete three weeks of ageing has in this figure been multiplied by a factor of 3.

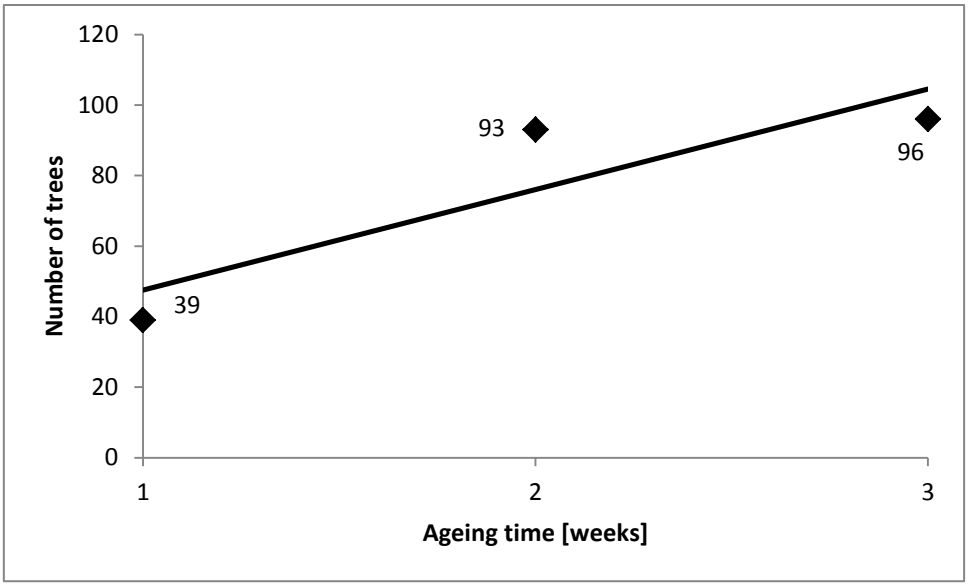

Figure 5.17. Aggregated number of observed vented and bow-tie water trees as a function of time. Test objects were exposed to a DC voltage with a superimposed high frequency AC component.

After one week of ageing, the observed water trees had an average length of 229.5 µm, with a standard deviation of 120.6 µm. Another week of ageing resulted in an observed average length of 230.4 µm and a standard deviation of 92.6 µm. After three weeks of ageing, the average aggregated water length was 285.2 µm, with a standard deviation of 138.9 µm. The average aggregated water tree length as a function of the ageing time can be seen below in figure 5.18.

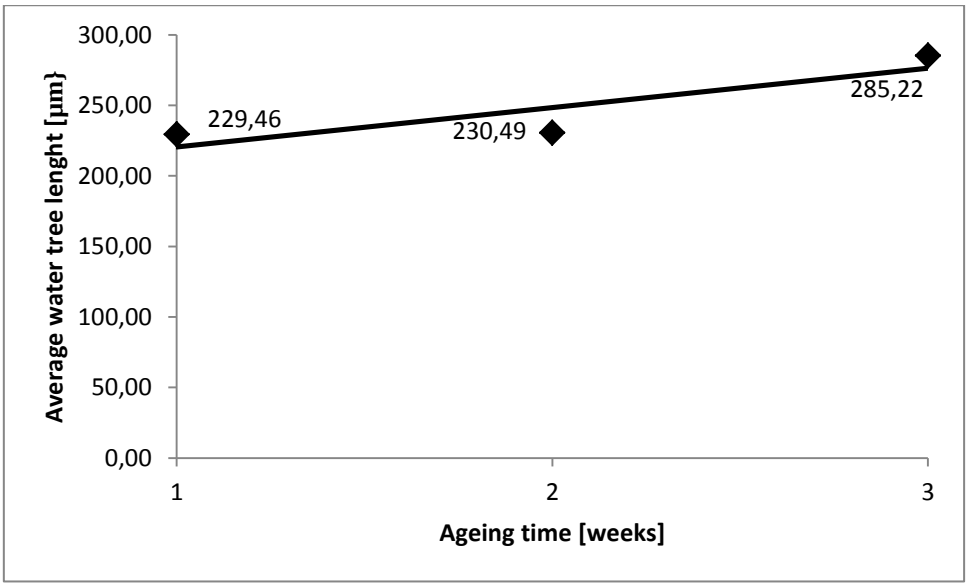

Figure 5.18. Average aggregated water tree length as a function of time. Test objects were exposed to a DC voltage with a superimposed high frequency AC component.

6. Discussion

6.1. High Frequency AC Component

All test objects exposed to a high frequency AC component experienced water tree initiation and growth during ageing. The length of the longest observed water tree increased with an increasing ageing time, confirming previous research [7]. The longest tree after two weeks of ageing was just marginally longer than the longest tree after one week of ageing. However, the longest tree after three weeks of ageing was 27% longer compared to the longest water tree observed after two weeks of ageing. This water tree measured 607 µm, corresponding to 55% of the total insulation thickness.

Two of the three respective water trees were bow-tie water trees. As mentioned in chapter 3, bow-tie water trees generally have a rapid initial growth, which then declines quickly. This could support the factum that many of the long water trees are bow-tie water trees, and also the fact that the observed growth has stagnated after the first week. However, some of the observed vented water trees were of almost comparable length to these bow-tie trees. These vented water trees could, with prolonged ageing, have led to a breakdown. Because the first test objects were removed after one complete week of ageing it is hard to say anything concrete about the water tree inception time.

The number of observed bow-tie water trees increased with an increasing duration of ageing. This increase, combined with the declining average bow-tie water tree length, and an increasing relative standard deviation, indicated a continuous initiation of new bow-tie water trees.

A significant number of vented water trees were observed in the test objects. After one week of ageing, all but one of the 22 observed vented water trees had been initiated at the upper semiconductor. The number of observed vented water trees from the upper semiconductor remained quite stable, numbering 34 after two weeks and 26 after three weeks of ageing. The average length of the vented water trees from the upper semiconductor was of comparable size after the first and the second week of ageing. However, after three weeks of ageing, there was a slight increase in the average length. The standard deviation was practically the same for all three ageing durations. This indicates an early initiation and quick initial growth rate, with a slower growth and a lower rate of initiation as the ageing continued past the first week.

As mentioned in chapter three, impurities on the interface between semiconductor and insulation can act as preferential sites for water tree initiation and significantly increase the initiation rate of vented water trees. The amount of vented water trees observed from the upper semiconductor, combined with observations made in the microscope, have indicated that there might be a problem with the old casting molds used in this master thesis and that these have resulted in irregularities and impurities on the interface between upper semiconductor and the insulation. Figure 6.1 gives an example of such an impurity.

Figure 6.1. Impurity and resulting vented water tree from upper semiconductor.

Only one vented water tree was observed from the lower semiconductor after one week of ageing. After two weeks of ageing a total of six water trees were observed. Five of these trees were observed in one test object. However, after three weeks of ageing, the number had increased drastically, and a total of 35 vented water trees were observed from the lower semiconductor. All three test objects aged for three weeks experienced vented water tree growth from the lower semiconductor, with the respective numbers being; 12, 16 and 5 water trees. One plausible explanation is that the initial saturation time of four weeks was insufficient and that the required humidity needed for the initiation of vented water trees at the lower semiconductor might have been attained during the ageing process. The average length after three weeks of ageing was 170.9 µm, with a standard deviation of 74.8 µm. This indicates a large dispersion, as the standard deviation is almost 44% of the average water tree length. The average length is also much lower compared to the venter water trees initiated at the upper semiconductor. This further strengthens the assumption made on lacking saturation.

The insufficient initial saturation at the lower semiconductor, combined with the impurities observed on the upper semiconductor, makes it hard to evaluate the effect of the salt particles. However, the exponential increase in the initiation of vented water trees from the lower semiconductor between two and three weeks of ageing gave an indication of the effect salt particles could have had under more optimal conditions.

As seen in figure 6.2, bow-tie water trees and vented water trees from the lower semiconductor constituted the main contribution to the increasing number of observed water trees during the ageing process. This further emphasizes the factum that impurities and the unsaturated insulation might have led to the initial vented water trees from the upper semiconductor, but as the ageing time increased, new water trees were formed within the insulation as bow-tie water trees or as vented water trees at the preferential sites created by the salt particles at the lower semiconductor.

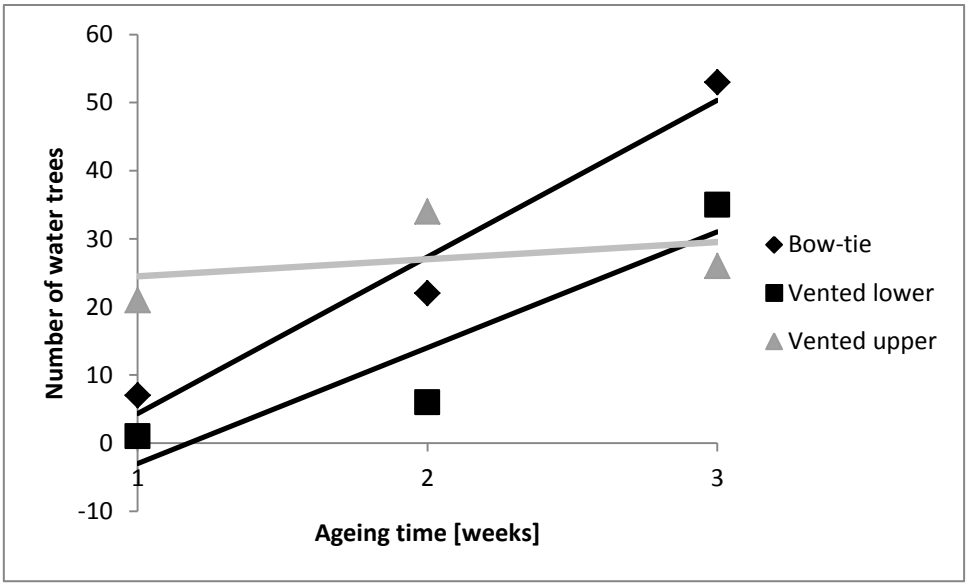

Figure 6.2. Number of observed water trees by type as a function of time. Test objects were exposed to a high frequency AC component only.

The aggregated number of observed water trees experienced an almost linear increase during the ageing process. There was also a decline in the average water tree length, while the standard deviation remained approximately the same for one and two weeks of ageing. This means that the respective standard deviation given as a percentage, increased from 35.5% to 40.1%. After three weeks of ageing, the average length was 257.4 µm, with a standard deviation of 122.9 µm, accounting for 48% of the average water tree length. The increasing dispersion and the declining average water tree length is a result of the continuous initiation of new water trees and the slow growth of the existing water trees.

6.2. DC Voltage with Superimposed High Frequency AC Component

All test objects exposed to a DC voltage with a superimposed high frequency AC component experienced water tree initiation and growth. However, two out of three test objects experienced breakdown before completing three weeks of ageing. This greatly reduced the number of investigated cuts from test objects subjected to three complete weeks of ageing and reduced the statistical credibility of these results. To make linear regression possible, the number of water trees found in the only test object aged for the complete period of three weeks had to be multiplied by 3. This crude simplification and has to be kept in mind when evaluating the experimental results for three weeks of ageing.

A slight reduction in the length of the longest observed water tree was experienced between one and two weeks of ageing. The decline corresponded to 10% of the length, and although minor, contradicts with previous research [7]. It has been assumed that this error is a result of the small sample pool. Additionally, the only test object to complete three weeks of ageing contained water trees above 600 µm, while the two other test objects experienced breakdown before completing three weeks of ageing. The breakdowns were most likely a result of a water tree bridging the insulation, having grown to 1100 µm, which is 100% of the total insulation thickness. This indicates that the length of the longest observed water tree increased with an increasing ageing time. It is uncertain whether the breakdowns were caused by vented water trees, bow-tie water trees, or water trees growing into each other, but it clearly indicates the dangers related to water tree

initiation and growth, and also that an ageing duration of three weeks was more than sufficient for experiments on Rogowski style test objects with an insulation thickness of 1.1 mm.

Bow-tie water trees and vented water trees from the upper semiconductor were observed in all test objects subjected to a DC voltage with a superimposed high frequency AC component. The number of bow-tie water trees and the number of vented water trees from the upper semiconductor were both found to increase with the duration of ageing. As a result of more water trees being initiated, they also experienced a decreasing average water tree length. A significant increase in the standard deviation was observed for both bow-tie water trees and vented water trees from the upper semiconductor from two to three weeks of ageing. By using bow-tie water trees as an example, one can see that the standard deviation increased with 116% between two and three weeks of ageing. This indicates a high dispersion and reduces the confidence one can have in the experimental results for three weeks of ageing and is a direct consequence of having only one test object subjected to three complete weeks of ageing. Many of the observed vented water trees initiated at the upper semiconductor were a result of imperfections on the interface between semiconductor and insulation.

Vented water trees from the lower semiconductor were observed to be dominant for all three periods of ageing. This was arguably a direct result of the hydrophilic sodium chloride particles acting as preferential sites for water tree initiation and growth. The vented water trees from the lower semiconductor were also observed to have a lower average tree length and a higher relative standard deviation compared to vented water trees from the upper semiconductor. This is a result of the accelerated water tree initiation rate, with new trees leading to a lower average water tree length and a higher dispersion.

The aggregated number of observed water trees was observed to increase with the duration of ageing. Between one and two weeks of ageing, the number increased with 138%. Between two and three weeks there was only a minor increase, but this was arguably a result of the small sample pool for three weeks of ageing, as the number of water trees observed in the only test object to complete three weeks of ageing was similar to the number observed in the test objects subjected to two weeks of ageing. Two more test objects would most likely have resulted in a larger increase in the aggregated number of observed water trees. Although the number of vented water trees from both the upper and lower semiconductor, as well as the number of bow-tie water trees increased with an increasing ageing duration, figure 6.4 clearly illustrates how vented water trees from the lower semiconductor formed the main contribution to the aggregated number of observed water trees. This was probably a direct consequence of the hydrophilic salt particles. The number of observed water trees for the only test object to complete three weeks of ageing has in this figure been multiplied by 3.

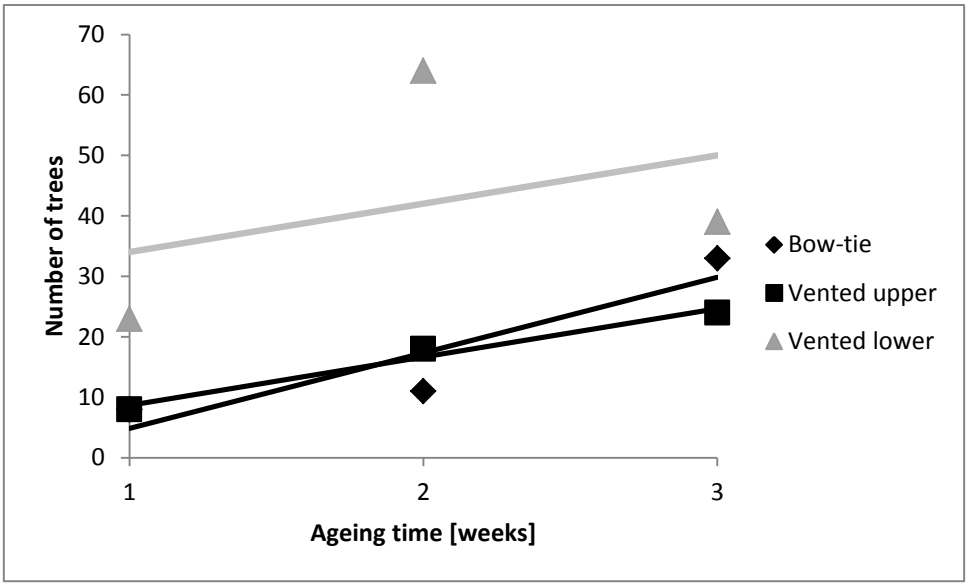

Figure 6.3. Number of observed water trees by type as a function of time. Test objects were exposed to a DC voltage with a superimposed high frequency AC component.

The average aggregated water tree length was observed to increase with an increasing duration of ageing. The increase was negligible between one and two weeks of ageing, while it was observed to increase greatly between two and three weeks of ageing. The increase in standard deviation indicates the problem with such a small sample pool for three weeks of ageing yet again, and it should be pointed out that the continuous initiation of new water trees combined with a slow existing water tree growth should have resulted in a quite stable, if maybe declining, average aggregated water tree length.

6.3. Comparison of Results

Both sets of experiments resulted in significant water tree initiation and growth. Additionally, both the length of the longest water tree and the aggregated water tree density were observed to increase with an increasing duration of ageing. The water trees from both sets of experiments were also of comparable form. All water trees were oblong and grew in the direction of the electrical field. Some bow-tie water trees were especially oblong, and seemed to consist of only one or two strings of micro voids. This corresponds with previous research [13] and is a direct result of the high frequency of the AC component. The two breakdowns experienced during testing with a DC voltage with a superimposed high frequency AC component greatly reduced the statistical credibility of the results for three weeks of ageing. As a result, when comparing the two sets of experiments, the two first weeks of ageing have been emphasized.

After one week of ageing the longest observed water tree was 12 % longer in the test objects exposed to a DC voltage and a superimposed high frequency AC component, compared to the test objects subjected to a high frequency AC component only. By assuming that the breakdowns were caused by water trees bridging the insulation, this difference increased to 81% after three weeks of ageing. The average aggregated length of the observed water trees was however lower for the experiments conducted with a DC voltage and a superimposed high frequency AC component, but this was arguably just a consequence of the higher water tree initiation rate. It should also be noted that the length of the longest water tree is most important when considering the consequences of water tree degradation. Even though the average water tree length might be small, one long water

tree bridging the insulation is enough to cause a breakdown. Figure 6.4 below presents the length of the longest observed water tree for the two sets of experiments as a function of time.

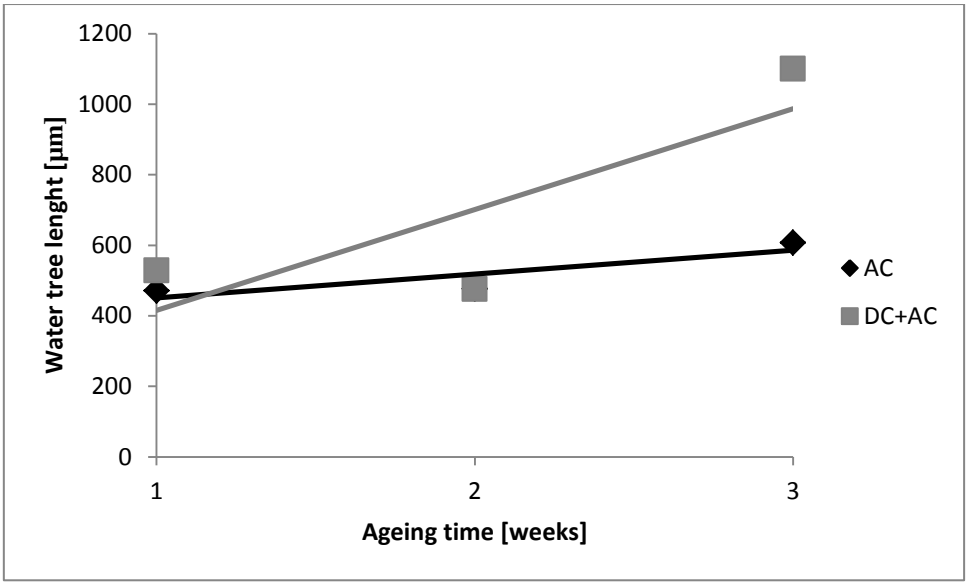

Figure 6.4. The longest observed water tree in each of the two sets of experiments as a function of time.

The DC component was observed to induce a higher water tree initiation rate. When comparing test objects subjected to one week of testing, the test objects subjected to a DC voltage with a superimposed high frequency AC component were observed to experience 34% higher water tree density. This percentage increased to 50% after two weeks of ageing. Vented water tree growth at the lower semiconductor was observed as the most significant difference between the two sets of experiments. The experiments conducted with a DC component with a superimposed high frequency AC component experienced significant vented water tree initiation at the lower semiconductor during the first week of ageing. In comparison, experiments conducted with a high frequency AC component only, experienced a significant initiation of vented water trees at the lower semiconductor between two and three weeks of ageing. Figure 6.5 illustrates the difference in the number of observed vented water trees at the lower semiconductor between the two sets of experiments as a function of the ageing time. The number of observed vented water trees from the lower semiconductor in the only test object to complete three weeks of ageing exposed to a DC voltage with a superimposed high frequency AC component has in this figure been multiplied by 3.

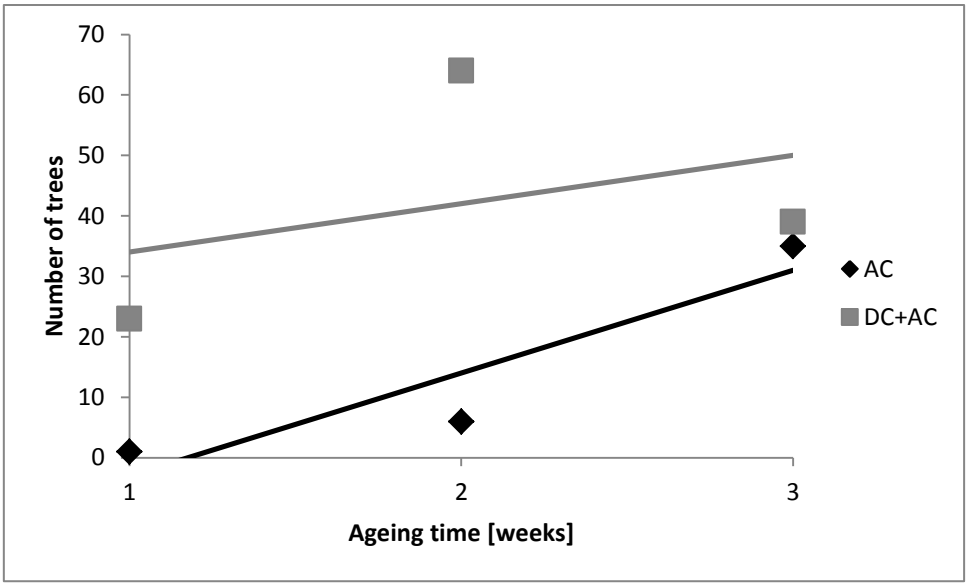

Figure 6.5. The number of vented water trees initiated at the lower semiconductor in each of the two sets of experiments as a function of time.

As mentioned in chapter three, the two requirements for water tree initiation and growth are the application of an AC voltage and the presence of electrolyte, which in this case was demineralized water. Both sets of experiments were conducted under near identical conditions, with the only difference being the DC component. The mechanism for the increase in water tree initiation and growth due to the DC component has not been fully understood. One theory is that the DC component has resulted in local field amplification at the salt particles and thus facilitated a faster saturation. The result is earlier water tree initiation, leading to a higher number of vented water trees from the lower semiconductor, and an overall higher aggregated number of water trees compared to the experiments conducted with a high frequency AC component only. As a result of this, in addition to the two breakdowns experienced, it could be argued that a DC component, in combination with a superimposed high frequency AC component, increases water tree degradation within XLPE insulation. This contradicts with earlier research [20].

All test objects were produced identically; with the same equipment and the same materials. Additionally, test objects showing any visual irregularities or imperfections were discarded. This means that the variations between individual test objects were small. However, some variations between the individual test objects might have occurred, and can have had an impact on the experimental results. In addition, significant imperfections were observed with the microscope at the upper semiconductor, and these have arguably acted as preferential sites for vented water tree initiation and facilitated vented water tree growth at this interface. This was an issue for all test objects, and cannot be said to have an impact on the comparison between the two sets of experiments.

7. Conclusion

The main objective of this master thesis was to study water tree degradation within wet XLPE insulation with relevant voltage stresses applied. An experimental setup capable of applying a DC voltage with a superimposed high frequency AC component was used to simulate the HVDC component and the overlaid transients that occur close to the power electronics used for AC to DC conversion. Rogowski shaped test objects with an insulation thickness of 1.1 mm and with 20 sodium chloride particles added at the lower semiconductor were tested. Two sets of experiments were conducted. The first set was conducted using a ± 2.05 kV/mm high frequency AC component only. The frequency of the AC component was 15 kHz. The second set of experiments was conducted combining the same high frequency AC component with a superimposed 12 kV/mm DC component. All other aspects of the experiments, including the test objects, were identical.

The experiments conducted with a high frequency AC component resulted in water tree initiation and growth. The length of the longest observed water tree was found to increase with an increasing duration of ageing, with the longest observed water tree after three weeks of ageing measuring 607 µm, corresponding to 55% of the total insulation thickness. The aggregated number of water trees was also observed to increase with an increasing ageing time. However, as a result of impurities on the upper semiconductor and insufficient saturation, most of the water trees observed in the test objects were either bow-tie water trees or vented water trees from the upper semiconductor. A significant increase in the number of vented water trees observed from the lower semiconductor from two to three weeks of ageing gave an indication on the effect the salt particles could have had under more optimal conditions.

Experiments conducted with a DC voltage and a superimposed high frequency AC component gave many similar results. The length of the longest observed water tree and the aggregated number of water trees were both found to increase with an increasing ageing time. Additionally, two out of three test objects suffered breakdown before completing three weeks of ageing. This was most likely the result of water trees bridging the 1100 µm thick insulation. It is uncertain if the breakdowns were caused by vented water trees, bow-tie water trees, or water trees growing into each other, but it clearly indicates the dangers related to water tree initiation and growth, and that the ageing duration of three weeks was more than sufficient.

After one week of ageing, a 34 % higher water tree density was observed in the test objects subjected to a DC voltage with a superimposed high frequency AC component compared to the test objects exposed to a high frequency AC component only. This percentage increased to 50 % after two weeks of ageing. Vented water tree growth at the lower semiconductor was the most significant difference between the two sets of experiments. One plausible theory is that the DC component has resulted in local field enhancement at the salt particles, facilitating faster saturation, and faster water tree initiation, leading to a higher number of vented water trees at the lower semiconductor, and a higher aggregated number of water trees. Due to the higher water tree density, in addition to the two breakdowns experienced, it could be argued that a DC component, when combined with a superimposed high frequency AC component, increases water tree degradation within wet XLPE insulation. The experiments also indicate that HVDC cables should be made water tight to prevent water tree growth due to the transients originating from the switching of the power electronics.

8. Further Studies

There are many possibilities for further studies on water tree degradation within wet XLPE insulation. The experiments covered in this master thesis have shown how transients with and without a DC component can result in water tree initiation and growth, and have indicated that a DC component, when combined with a superimposed AC component, can increase water tree degradation.

The statistical quality and the quantity of data are always of great importance when discussing experimental results. Two out of three test objects exposed to a DC voltage with a superimposed high frequency AC component suffered breakdown before completing three weeks of ageing. This greatly reduced the sample pool and the validity of the results for three weeks of ageing. New experiments should be conducted with an ageing duration of three weeks. By reducing the ageing duration to five, ten and fifteen days respectively, it might be possible to avoid breakdown all together. This is recommended as breakdowns were experienced both during this master thesis and also during previous research using Rogowski shaped test objects [12].

Impurities were observed on the upper semiconductor and these have arguably acted as preferential sites for water tree initiation and increased the initiation rate of vented water trees from the upper semiconductor. Observations made in the microscope have indicated that there might be a problem with the old casting molds used in this master thesis and conducting new experiments, using new casting molds, should increase the quality of the experimental results.

Lacking saturation throughout the insulation was another issue in this master thesis. This can be avoided by increasing the preconditioning period with demineralized water. Eight weeks of preconditioning should ensure complete saturation throughout the insulation and could make it easier to evaluate the effect of the salt particles. Another possibility is to perform two sets of near identical experiments, using one set of Rogowski test objects with salt particles and one set of Rogowski test objects without salt particles. This could also make it easier to evaluate the effect of adding hydrophilic groups and “virtual” imperfections to the insulation.

Ultimately, the quantity and quality of the experimental results are the most critical parameters for laboratory research, and further studies are encouraged to validate and increase the credibility of the experimental results.

Bibliography

[1] European Commission. (2013, April) EU Policy on Climate Change. [Online]. http://ec.europa.eu/clima/policies/brief/eu/index_en.htm

[2] Forewind. (2013, April) Forewind Fact Sheet. [Online]. http://www.forewind.co.uk/uploads/files/10898_FOR_Gen_Factsheet_v7_Hires.pdf

[3] The Regional Group North Sea for the NSCOGI, "Offshore Transmission Technology," ENTSOE, Brussels, 2011.

[4] N Mohan, T. M Undeland, and W. P Robbins, *Power Electronics; Converters, Applications, and Design*.: John Wiley and Sons, 2003.

[5] Gunnar Asplund et al., "DC Transmission Based on Voltage Source Converters," in *CIGRE Session* , Paris, 1998, pp. 14-302.

[6] Thomas Blooming and Daniel J Carnovale, "Application of IEE STD 519-1992 Harmonic Limits," in *Pulp and Paper Industry Technical Conference, 2006. Conference Record of Annual* , Appelton, 2006, pp. 1-9.

[7] F Mauseth, M Amundsen, and H Faremo, "Water Tree Growth of Wet XLPE Cables Stressed with DC and High Frequency AC Voltage Superimposed," in *Electrical Insulation (ISEI), Conference Record of the 2012 IEEE International Symposium on* , San Juan, 2012, pp. 266-269.

[8] Blandine Hennuy et al., "Water Trees in Medium Voltage XLPE Cables: Very Short Time Accelerated Ageing Tests," in *Electricity Distribution - Part 1, 2009. CIRED 2009. 20th International Conference and Exhibition on* , Prague, 2009, pp. 1-4.

[9] E Ildstad, H Bårdsen, H Faremo, and B Knutsen, "Influence of Mechanical Stress and Frequency on Water Treeing in XLPE Cable Insulation," in *Electrical Insulation, 1990., Conference Record of the 1990 IEEE International Symposium on* , Toronto, 1990, pp. 165-168.

[10] R Ross, "Inception and Propagation Mechanisms of Water Treeing," *IEEE Transactions on Dielectrics and Electrical Insulation*, vol. 5, no. 5, pp. 660-680, August 2002.

[11] Erling Ildstad, *High Voltage Insulation Materials*. Trondheim: NTNU, 2012.

[12] Andreas Lind, "Innvirkning av HVDC-komponent med overlagrede transienter på vanntrevekst i PEX-isolasjon," NTNU, Trondheim, Master Thesis 2012.

[13] J. C Fothergill, A Eccles, J. A Houlgreave, and L. A Dissado, "Water tree inception and its dependence upon electric field, voltage and frequency," *Science, Measurement and Technology, IEE Proceedings A*, vol. 140, no. 5, pp. 397-403, September 1993.

[14] Erling Ildstad, *Cable Technology*. Trondheim: NTNU, 2009.

[15] GSM Industries. [Online]. http://www.gsmindustries.co.in/pages/products/plastic-extruder-machinery.html

[16] F Mauseth, M Amundsen, A Lind, and H Faremo, "Water Tree Growth of Wet XLPE Insulation Stressed with DC and High Frequency AC," in *Electrical Insulation and Dielectric Phenomena (CEIDP), 2012 Annual Report Conference on* , Montreal, 2012, pp. 692-695.

[17] Petter I Nodeland, "Utvikling av testoppsett for spenningsprøving av HVDC PEX-kabler - Innvirkning av HVDC med overlagrede transienter på levetiden," NTNU, Trondheim, Master Thesis 2010.

[18] Martin Amundsen, "Aldring av PEX-isolasjon ved påtrykk av HVDC med overlagrede transienter," NTNU, Trondheim, Master Thesis 2012.

[19] Michael P Bahrman, Jan G Johansson, and Bo A Nilsson, "Voltage Source Converter Transmission Technologies - The Right Fit for the Application," in *Power Engineering Society General Meeting, 2003, IEEE (Volume:3)* , Toronto, 2003, p. Volume 3.

[20] Hans H Sæternes, Jørund Aakervik, and Sverre Hvidsted, "Water Treeing in XLPE Insulation at a Combined DC and High Frequency AC Stress," in *2013 IEEE Electrical Insulation Conference (EIC)*, Ottawa, 2013.

Appendix

A. High Frequency AC Component

Ageing time [hours]	Test object	Bow-tie	Vented upper s.c.	Vented lower s.c.
168	1A	3	8	1
168	1B	-	6	-
168	1C	4	7	-

Ageing time [hours]	Test object	Bow-tie	Vented upper s.c.	Vented lower s.c.
336	2A	3	11	5
336	2B	10	11	1
336	2C	9	12	-

Ageing time [hours]	Test object	Bow-tie	Vented upper s.c.	Vented lower s.c.
504	3A	18	10	12
504	3B	22	11	16
504	3C	13	7	5

B. DC Voltage with Superimposed High Frequency AC Component

Ageing time [hours]	Test object	Bow-tie	Vented upper s.c.	Vented lower s.c.
168	1A	3	4	5
168	1B	4	2	13
168	2C	1	6	5

Ageing time [hours]	Test object	Bow-tie	Vented upper s.c.	Vented lower s.c.
336	2A	3	9	13
336	2B	1	5	25
336	2C	7	4	26

Ageing time [hours]	Test object	Bow-tie	Vented upper s.c.	Vented lower s.c.
388	3A – Breakdown	-	-	-
391	3B – Breakdown	-	-	-
504	3C	11	8	13